

Faddeev calculation of 3 and system s using resonating-group method kernel

Y. Fujiiwara

Department of Physics, Kyoto University, Kyoto 606-8502, Japan

K. Miyagawa

Department of Applied Physics, Okayama Science University, Okayama 700-0005, Japan

M. Kohno

Physics Division, Kyushu Dental College, Kitakyushu 803-8580, Japan

Y. Suzuki

Department of Physics, Niigata University, Niigata 950-2181, Japan

D. Baye

Physique Nucléaire Théorique et Physique Mathématique,
CP 229, Université Libre de Bruxelles, B-1050 Brussels, Belgium

J.-M. Sparenberg

TRIUMF, 4004 Wesbrook Mall, Vancouver, British Columbia, Canada V6T 2A3

(Dated: May 23, 2019)

We carry out Faddeev calculations of three-alpha (3) and two-alpha plus (+) systems, using two-cluster resonating-group method kernels. The input includes an effective two-nucleon force for the resonating-group method and a new effective N force for the interaction. The latter force is a simple two-range Gaussian potential for each spin-singlet and triplet state, generated from the phase-shift behavior of the quark-model hyperon-nucleon interaction, fss2, by using an inversion method based on supersymmetric quantum mechanics. Owing to the exact treatment of the Pauli-forbidden states between the clusters, the present three-cluster Faddeev formalism can describe the mutually related, 3 and + systems, in terms of a unique set of the baryon-baryon interactions. For the three-range Minnesota force which describes the phase shifts quite accurately, the ground-state and excitation energies of ^9Be are reproduced within 100–200 keV accuracy.

PACS numbers: 21.45.+v, 21.30.-x, 13.75.Cs, 12.39.Jh

I. INTRODUCTION

In spite of much effort to incorporate microscopic features of the alpha-alpha (+) interaction, a consistent description of the three-alpha (3) and two-alpha plus (+) systems has not yet been obtained so far in the Faddeev formalism. The most favorable description of the system is the resonating-group method (RGM) [1]. Although some of the previous works deal with the RGM kernel explicitly in the 3-cluster Faddeev formalism, they usually yield a large overbinding for the ground state and sometimes involve spurious states because of an incomplete treatment of the Pauli-forbidden states in the 3 model space [2–5]. Various types of 3 orthogonality condition models (OCM) [6–8] also yield a similar overbinding for the ground state, although the effect of the Pauli principle between clusters is satisfactorily treated in each framework. Only one exception for this rule is the 3 OCM in Refs. [9, 10], in

which the Pauli forbidden components described by the bound-state solutions of the deep Buck, Friedrich, and Wheatley (BFW) potential [11] is completely eliminated. The result is rather similar to the traditional 3 Faddeev calculation using Ali-Bardem phenomenological potential with a repulsive core [12]. In these calculations, the ground-state energy of the 3 system is less than 1.5 MeV, and a simultaneous description of the compact shell-model-like ground state and the excited 0^+ state with well-developed cluster structure is not possible. The origin of the different conclusions in Refs. [8] and [9, 10], is spelled out in Ref. [13], in which the existence of almost forbidden Faddeev components inherent to this 3 OCM using the bound-state Pauli-forbidden states of the BFW potential is essential.

A possible resolution of this overbinding problem of the 3 model is found in our new three-cluster Faddeev formalism, which uses singularity-free T-matrices (RGM T-matrices) generated from the two-cluster RGM kernels [14]. In this formalism, solving the Faddeev equation automatically guarantees the elimination of the three-cluster redundant components from the total wave function. The explicit energy dependence inherent in the ex-

Electronic address: fujiwara@ruby.scp.phys.kyoto-u.ac.jp

change RGM kernel is self-consistently treated. We first applied this formalism to the three-dineutron and 3 systems, and obtained complete agreement between the Faddeev calculations and variational calculations using the translationally invariant harmonic-oscillator (h.o.) basis [14, 15]. Next, this formalism was applied to a Faddeev calculation of the three-nucleon bound state [16], which employs complete one-shell Γ -matrices derived from the non-local and energy-dependent RGM kernels of the quark-model NN interactions, FSS [17] and fss2 [18]. The fss2 model yields a triton binding energy $B_t = 8.519$ MeV in the 50 channel calculation, when the np interaction is employed for all the NN pairs in the isospin basis [19]. The effect of the charge dependence of the two-body NN interaction is estimated to be 0.19 MeV for the triton binding energy [20]. This implies that our result is not overbinding in comparison with the empirical value, $B_t^{\text{exp}} = 8.48$ MeV. If we attribute the difference, 0.15 MeV, to the effect of the three-nucleon force, it is by far smaller than the generally accepted values, 0.5–1 MeV [21], predicted by many Faddeev calculations employing modern realistic meson-theoretical NN interactions. We have further applied this three-cluster Faddeev formalism to the hypertriton system [22], in which the quark-model hyperon-nucleon (YN) interactions of fss2 yield a reasonable result of the hypertriton properties similar to the Nijmegen soft-core potentials NSC 89 [23], NSC 97f and NSC 97e [24]. Most mathematical details for the Faddeev equation, employed in this calculation, are given in the present paper.

Here we apply the present three-cluster Faddeev formalism to the model for ${}^9\text{Be}$. This hypernucleus plays an important role to study the N interaction in the p-shell hypernuclei. From the early time of the hypernuclear study, ${}^9\text{Be}$ is considered to be a prototype of -cluster structure, in which the two clusters form a loosely bound subsystem by the effect of the extra hyperon [25]. Since the YN interaction is usually weaker than the NN interaction, this system is suitable for studying a subtle structure change of the two- system from ${}^8\text{Be}$. In fact, in addition to the $1=2^+$ ground state [26][29] with the Δ -separation energy $B({}^9\text{Be}) = 6.71 \pm 0.04$ MeV [30], the recent γ -ray spectroscopy [31] has revealed the existence of two narrow resonances in the excited states, which are supposed to be $5=2^+$ and $3=2^+$ states generated from the small spin-orbit splitting in the weak coupling picture of ${}^8\text{Be}(2^+)$ (spin $S = 1=2$). From a theoretical point of view, this is the simplest non-trivial system which requires the Faddeev formalism with two identical particles, involving three Pauli-forbidden states at the two-cluster level. Several model calculations were already done with various frameworks and two-body potentials. Hiyama et al. [7] used the OCM for the , 3 and system and discussed not only the ground state of ${}^9\text{Be}$, but also the spin-orbit splitting of the $5=2^+$ and $3=2^+$ states [32]. They employed simple three-range Gaussian potentials for the N interaction [33] based on Γ -matrix calcu-

lations of various Nijmegen and Jülich YN one-boson-exchange-potential (OBEP) models. The potentials are generated from these effective potentials by the folding procedure with respect to the $(0s)^4$ h.o. wave function of the cluster. They introduced a three-force and adjusted the YN parameters to reproduce the binding energies of the ${}^{12}\text{C}$ and ${}^9\text{Be}$ ground states. Filkin and Gal [34] used the Faddeev and Faddeev-Yakubovsky formalisms to calculate the ${}^9\text{Be}$ and ${}^{10}\text{Be}$ ground states. They used the Al-Bodmer potential [12] and the so-called Isle potential [35] for the interaction. They included only S-wave in the calculation, and reproduced the ${}^9\text{Be}$ ground-state energy correctly. However, if one includes higher partial waves the Al-Bodmer potential yields overbinding for ${}^9\text{Be}$ by more than 0.5 MeV. Oryu et al. [36] carried out a Faddeev calculation by using the RGM kernel and various types of potentials in the separable expansion method. Their energy spectrum of ${}^9\text{Be}$ is reasonable, but the treatment of the two- Pauli principle in the system is only approximate. Since they neglected the Coulomb force, a detailed comparison between their calculated results and experiment is not possible. Koike [37] also performed and in Faddeev calculations in the complex energy method, in order to find a new structure like ${}^5\text{He}$ in the continuum region.

Our purpose for the Faddeev calculations using RGM kernels is threefold. First, we develop a general three-cluster Faddeev formalism with two identical clusters, in order to apply it to more complex three-cluster systems like the hypertriton interacting via quark-model baryon-baryon interactions. In the hypertriton system, we have to deal with the NN – NN coupled-channel system which involves a Pauli-forbidden state at the quark level in the NN subsystem. Since the baryon-baryon interactions in the quark model are formulated in the two-cluster RGM formalism, the present three-cluster formalism is most appropriate to correlate the baryon-baryon interactions with the structure of few-baryon systems. The second purpose is to make a consistent description of the , 3 and systems using effective NN and N interactions. This attempt is beyond the scope of the usual OCM framework and the Faddeev formalism assuming only inter-cluster potentials. A comparison of the present 3 results with the fully microscopic 3 RGM or GCM [38][40] is useful to examine the approximations involved in the present three-cluster formalism. The third purpose is to present a tractable effective N force for cluster calculations of various p-shell hypernuclei, which is not purely phenomenological but derived microscopically from quark-m model baryon-baryon interactions. In particular, this effective N force should be able to reproduce the correct Δ -separation energy of ${}^5\text{He}; \text{B}({}^5\text{He}) = 3.12 \pm 0.02$ MeV. Such an interaction is indispensable for, e.g., a Faddeev calculation using the quark-m model interaction. In this paper, we derive an effective N force of two-range Gaussian form from the phase-shift behavior of the quark-m model YN

interaction, fss2, by using an inversion method based on supersymmetric quantum mechanics [41].

This paper is organized as follows. In the next section, the three-cluster Faddeev formalism with two identical clusters is given, together with expressions to calculate the expectation values of the two-cluster Hamiltonian with respect to the solutions resulting from the Faddeev equation. The procedure to calculate the and T -matrices is also discussed, as well as the treatment of the cut-off Coulomb force employed in this paper. In the third section, we first briefly discuss the results of the 3 Faddeev calculation, and then those of the Faddeev calculation. The final section is devoted to a summary. Appendix A gives some basic formulas for the rearrangement factors of three-body systems with two identical particles. The most general case with explicit spin-isospin degrees of freedom is discussed. In Appendix B, we derive a compact formula to calculate the Born kernel for arbitrary types of N interactions. The Born kernel of the RGM is given in Appendix C. Energies are in MeV and lengths in fm throughout.

II. FORMULATION

A. Faddeev equation for systems with two identical clusters

In order to formulate the Faddeev equation for systems with two identical particles, we follow the notation of Ref. [42] as much as possible. The Jacobi-coordinate vectors are specified by the permutation (\quad) , which is a cyclic permutation of (123). For example, the momentum vectors for the coordinate system in the unit of \sim are defined by

$$\begin{aligned} p &= \frac{m_1 \mathbf{k}_1 + m_2 \mathbf{k}_2}{m_1 + m_2}; \\ q &= \frac{1}{M} [(m_1 + m_2) \mathbf{k}_1 - m_1 (\mathbf{k}_1 + \mathbf{k}_2)]; \\ P &= \mathbf{k}_1 + \mathbf{k}_2 + \mathbf{k}_3; \end{aligned} \quad (1)$$

where $\mathbf{k}_1, \mathbf{k}_2, \mathbf{k}_3$ are single-particle momenta of particles 1, 2, 3 with the masses m_1, m_2, m_3 , respectively, and $M = m_1 + m_2 + m_3$ is the total mass. We choose the coordinate system $\sim = 3$ as the standard set of Jacobi coordinates and assume that particles 1 and 2 are the two identical particles with a common mass $m_1 = m_2$. Some examples are given in Table I for the assignment of particle numbers.

We incorporate the symmetry property for the exchange of particles 1 and 2 into the Faddeev formalism by assuming the total wave function $(p; q)$ as

$$(p_3; q_3) = (p_3; q_3) ' (p_1; q_1) + ' (p_2; q_2) \quad (2)$$

with $(p_3; q_3) = (p_3; q_3)$;

where the upper (lower) sign is applied for identical bosons (fermions). The requirement $(p; q) =$

$(p; q)$ is satisfied. The Faddeev components and $'$ are determined from

$$\begin{aligned} (p; q_3) &= G_0(p; q_3) \quad dp_3 \hbar p \mathbf{j}^F(E - h_3) \mathbf{j}_3 i \\ &\quad [(p_2; q_2) ' (p_1; q_1)] ; \\ ' (p; q_2) &= G_0(p; q_2) \quad dp_2 \hbar p \mathbf{j}^T(E - h_2) \mathbf{j}_2 i \\ &\quad [(p_3; q_3) ' (p_1; q_1)] ; \end{aligned} \quad (3)$$

where $G_0(p; q) = (E - H_0)^{-1}$ is the free Green function of the three-particle system with the negative energy $E < 0$, and $(p_3; q_3), (p_2; q_2), (p_1; q_1)$ are related to each other in the standard relationship for the rearrangement of Jacobi coordinates:

$$\begin{aligned} p &= \frac{m_1}{m_1 + m_2} \quad \frac{m_1 M}{(m_1 + m_2)(m_1 + m_3)} \quad p \\ q &= 1 \quad \frac{m_1}{m_1 + m_3} \quad q \end{aligned} \quad (4)$$

In Eq. (3), h_3 and h_2 stand for the free kinetic energies of the third particle, corresponding to the decomposition of the free three-body kinetic energy operator, $H_0 = h_1 + h_2$. The two-body T -matrices \mathbf{j}^F and \mathbf{j}^T sometimes include the energy dependence on $'$ and $''$ in the present three-cluster formalism, which will be discussed in the next subsection.

The rearrangement of the Jacobi coordinates in Eq. (3) involves some complication, together with the partial wave decomposition. These are deferred to Appendix A for the general expressions. Here we specify the system and only give the specification scheme of channels and the Faddeev equation after the partial-wave decomposition. We give expressions both in the LS-coupling and jj-coupling schemes for later convenience. For the ${}^9\text{Be}$ system, channels are specified as follows. The channel is defined by $\sim = 3$ with $(\quad) = (312)$. The Jacobi coordinates in this channel are

$$p_3 = \frac{1}{2} (\mathbf{k}_1 - \mathbf{k}_2); \quad q_3 = \frac{1}{8} [8\mathbf{k}_3 - (\mathbf{k}_1 + \mathbf{k}_2)]; \quad (5)$$

where \sim is the mass ratio of \sim to \sim ; $\sim = M_N$. The partial-wave decomposed state $(p_3; q_3)$ is and the

TABLE I: Assignment of particle numbers for three-cluster systems with two identical particles or clusters.

particle	mass	${}^9\text{Be}$	${}^6\text{He}$	${}^3\text{H}$	${}^3\text{H}$	${}^3\text{He}$
1	m_1			N	n	p
2	m_1			N	n	p
3	m_3			or	p	n

angular-spin wave functions $h_{\mathbf{p}_3; \mathbf{q}_3 j} i$ are given by

$$\begin{aligned} \dot{p}_3; q_3; i = \dot{p}_3; q_3; [(\text{h})^L 1=2] J J_z i; & \quad i \\ \dot{h} \dot{p}_3; \dot{q}_3; j = & \quad 1 \quad 2 \quad Y(\text{h})^L (\dot{p}_3; \dot{q}_3) \quad \frac{1}{2} (3) \quad J J_z \\ & \quad (\text{L S-coupling}); \quad (6a) \end{aligned}$$

Here, $Y_{\text{LLz}}(\mathbf{p}; \mathbf{q}) = [Y(\mathbf{p})Y(\mathbf{q})]_{\text{LLz}}$, $\frac{1}{2}$ (3) is the spin wave function of \downarrow , and \downarrow is the internal wave function of the particle. Similarly, we define the channel by $= 2$ with $(\quad) = (231)$. The Jacobi coordinates in this channel are

$$p_2 = \frac{1}{4+} (4k_3 - k_1) ;$$

$$q_2 = \frac{1}{8+} [(4+)k_2 - 4(k_3 + k_1)] ; \quad (7)$$

with the partial-wave decomposition

$$\begin{aligned}
 & \text{Left side: } \mathbf{p}_2; \mathbf{q}_2; \mathbf{i} = \mathbf{p}_2; \mathbf{q}_2; [\mathbf{h}\mathbf{h}^* \text{ (1=2)}] \mathbf{I} \mathbf{J}_2 \mathbf{J}_z \mathbf{i}; \quad \mathbf{i} \\
 & \text{Right side: } \mathbf{p}_2; \mathbf{q}_2 \mathbf{j} \mathbf{i} = \mathbf{Y}_1 \mathbf{p}_2 \mathbf{Y}_2 \mathbf{q}_2 \mathbf{j} \mathbf{i} \\
 & \quad (\text{jj-coupling}) : \quad (8b)
 \end{aligned}$$

The channel is specified by $\gamma = 1$ with $(\gamma) = (123)$. The Jacobi coordinates in this channel are given by

$$p_1 = \frac{1}{4+} (k_2 - 4k_3) ;$$

$$q_1 = \frac{1}{8+} [(4+)k_1 - 4(k_2 + k_3)] : \quad (9)$$

For the quantum numbers we use the same notation as that of the channel, by simply changing to p_1 and p_2, q_2 to p_1, q_1 . The partial-wave decomposition in the Dirac notation is carried out, for example, as

$$\dot{p}_i; q_i = \dot{p}_i; q_i; \text{ in } \dot{p}_i; q_i; \quad (10)$$

where in the summation specifies various quantum numbers in Eqs. (6) and (8). The partial-wave decomposition of the Faddeev equation for the two components and in Eq. (2) is given by

$$(p;q) = E \frac{\sim^2}{4M_N} p^2 + \frac{8+}{4} q^2 \int_0^1 q^0 dq^0 \int_1^Z dx h p \int_E^F E \frac{\sim^2}{4M_N} \frac{8+}{4} q^2 ;" \quad p_1 i$$

$$X \frac{1}{p_1} g (q; q^0; x) \frac{1}{p_2}, \quad (p_2; q^0); \quad (11a)$$

$$\begin{aligned}
 & \langle p; q \rangle = E \frac{\frac{1}{2} \int_0^1 q^2 dq^0}{8M_N} \left(\frac{4}{4+q^2} p^2 + \frac{8}{4+q^2} q^2 \right) \\
 & X \frac{1}{p_1^0} g(p_1^0; q^0; x) \frac{1}{p_2^0} = \langle p_2^0; q^0 \rangle + h(p_2^0; q^0) \\
 & E \frac{\frac{1}{2} \int_0^1 q^2 dq^0}{8M_N} \left(\frac{8}{4+q^2} q^2 \right) \frac{1}{p_1^0} g(p_1^0; q^0; x) \frac{1}{p_2^0} = \langle p_2^0; q^0 \rangle;
 \end{aligned}
 \quad (11b)$$

$$\text{where } \left(\begin{array}{l} p_1 = p \ q^0; \frac{1}{2}q; x \\ p_2 = p \ q; \frac{1}{4+}q^0; x \end{array} \right) ; \quad \left(\begin{array}{l} p_1^0 = p \ q^0; \frac{1}{4+}q; x \\ p_2^0 = p \ q; \frac{1}{2}q^0; x \end{array} \right) ; \quad \left(\begin{array}{l} p_1 = p \ q^0; \frac{4}{4+}q; x \\ p_2 = p \ q; \frac{4}{4+}q^0; x \end{array} \right) ; \quad (11c)$$

with $p(q; q^0; x) = \frac{p}{q^2 + q^{02} + 2q q^0 x}$. The T_m atrioes, T_0 and T_1 , are discussed in Subsecs. II.D and II.C. The rearrangement factors for the $-'$ or $'-$ cross terms are given by

$$g(q; q^0; x) = g(q^0; q; x) = \frac{x}{q^{\frac{0}{1} + \frac{0}{2}} - q^0 \frac{1}{1} + \frac{0}{2}} = \frac{\frac{1}{2}}{\frac{1}{2} + \frac{2}{4}} = \frac{\frac{1}{2}}{\frac{3}{4}} = \frac{2}{3} x^{\frac{0}{2}} (2k+1) g^{\frac{1}{1} - \frac{0}{1} k} P_k(x); \quad (12)$$

where $P_k(x)$ is the Legendre polynomial of rank k . The angular momentum factor $g^{1 \ 0 \ 1 \ k}$ is given by

$$g^{1 \ 0 \ 1 \ k} = G_{(\cdot \cdot);(\cdot \cdot)}^{1 \ 0 \ 1 \ k \ L} \quad (\text{LS coupling}) ;$$

$$= \frac{X}{L} \left(-1 \right)^{I+J+L+1+1} \frac{p}{2j+1} \frac{p}{2} \frac{b^2}{L} \frac{j}{J} \frac{1}{2} \frac{L}{I} \frac{1}{2} G_{(\cdot \cdot);(\cdot \cdot)}^{1 \ 0 \ 1 \ k \ L} \quad (\text{jj coupling}) ; \quad (13)$$

with $b = \frac{p}{2j+1}$, etc. The spatial angular momentum factor for the rearrangement, $G_{(\cdot \cdot);(\cdot \cdot)}^{1 \ 0 \ 1 \ k \ L}$, is given in Appendix Eq. (A 16). For the ' - ' type rearrangement, these are given by

$$g^{0 \ 0}(q; q^0; x) = \frac{X}{1+2} \frac{X}{1+2} \frac{q^{0+2} q^{0+2}}{q^{0+2} q^{0+2}} \frac{4}{4+} \frac{2+0}{k} (2k+1) g^{1 \ 0 \ 1 \ k} P_k(x) ; \quad (14)$$

with

$$g^{1 \ 0 \ 1 \ k} = \left(-1 \right)^{1+0} G_{(\cdot \cdot);(\cdot \cdot)}^{1 \ 0 \ 1 \ k \ L} \quad (\text{LS coupling}) ;$$

$$= \frac{X}{L} \left(-1 \right)^{I+0} \frac{p}{2j+1} \frac{p}{2} \frac{b^2}{L} \frac{J}{I} \frac{1}{2} \frac{L}{I} \frac{1}{2} G_{(\cdot \cdot);(\cdot \cdot)}^{1 \ 0 \ 1 \ k \ L} \quad (\text{jj coupling}) ; \quad (15)$$

B. Calculation of " and "

In this subsection, we derive some formulas to calculate expectation values of the two-cluster Hamiltonian, $h + V^{\text{RGM}}(")$, and $h + V$, where h is the kinetic-energy operator of the -pair etc. In the present application, $V^{\text{RGM}}(")$ is the RGM kernel and V is the kernel. We deal with the energy dependence of the RGM kernel self-consistently by calculating

$$" = h \ jh + V^{\text{RGM}}(") ji \quad (16)$$

for the normalized Faddeev solution . The potential term of the matrix element in Eq. (16) is most easily obtained from various matrix elements of the kinetic-energy operators. Suppose be a sum of three Faddeev components, $" = " + " + "$. Then the Faddeev equation $(E - H_0) " = V$ with $V = V^{\text{RGM}}(")$ and $H_0 = h + h$ yields $h \ jy \ j i = h \ jE \ H_0 \ j i$. Thus Eq. (16) becomes

$$" = E h \ j i h \ jH_0 \ j i + h \ jh \ j i : \quad (17)$$

We can write a similar equation also for the pair. We calculate " , although the self-consistent procedure is not necessary for the interaction. The kinetic energy term $h \ jh \ j i$ is obtained from $h \ jh \ j i$ as follows. Using the momentum Jacobi coordinates in Eq. (1), we can easily show

$$(m + m)h + (m + m)h + (m + m)h = M H_0 : \quad (18)$$

For two identical particles with $m = m$, this relationship yields

$$h + h = \frac{M}{m + m} H_0 - \frac{2m}{m + m} h ; \quad (19)$$

and

$$h \ jh \ j i = \frac{M}{2(m + m)} h \ jH_0 \ j i$$

$$+ \frac{m}{m + m} h \ jh \ j i : \quad (20)$$

Thus we find

$$" = E h \ j i + \frac{M}{2(m + m)} h \ jH_0 \ j i$$

$$+ \frac{m}{m + m} [h \ jH_0 \ j i - h \ jh \ j i] : \quad (21)$$

For the system , this expression is

$$" = E h \ j i + \frac{8+}{2(4+)} h \ jH_0 \ j i$$

$$+ \frac{4}{4+} [h \ jH_0 \ j i - h \ jh \ j i] : \quad (22)$$

We need to calculate the overlap matrix elements $h \ j i$, $h \ jH_0 \ j i$, and $h \ jh \ j i$, and

$$h \ jH_0 \ j i = h \ jH_0 \ j i + 2 h \ jH_0 \ j i ;$$

$$h \ jH_0 \ j i = h \ jH_0 \ j i + h \ jH_0 \ j i + i ;$$

$$h \ jh \ j i = h \ jh \ j i + 4 h \ jh \ j i$$

$$+ 2 h \ jh \ j i + i : \quad (23)$$

These are calculated from and ' by using the recoupling techniques developed in Appendix A . The final result is

$$\begin{aligned}
 h \text{ } \mathbb{H} \text{ } o \text{ } j \text{ } i = & \frac{x}{0} \frac{Z_1}{p^2 dp q^2 dq \frac{\sim^2}{4M_N}} \frac{p^2 + \frac{8+}{4} q^2}{[(p; q)]^2} \\
 + & \frac{x}{0} \frac{Z_1}{q^2 dq q^0 dq^0} \frac{Z_1}{1} \frac{dx}{(p_1; q) \frac{\sim^2}{4M_N}} \frac{p_1^2 + \frac{8+}{4} q^2}{[(p_1; q)]^2} \frac{1}{p_1} g \frac{(q; q^0; x) \frac{1}{p_2}}{(p_2; q^0)}; \quad (24a)
 \end{aligned}$$

$$\begin{aligned}
h \cdot J_0 \cdot j_i = & \frac{x}{0} \frac{Z_1}{p^2 dp q^2 dq} \frac{\sim^2}{8M_N} \frac{4+}{p^2} + \frac{8+}{4+} q^2 \cdot [(p; q)^2 \\
& + \frac{1}{2} \frac{x}{0} \frac{Z_1}{q^2 dq q^0 dq^0} \frac{Z_1}{dx} \cdot (p_1; q) \frac{\sim^2}{8M_N} \frac{4+}{p_1^2} + \frac{8+}{4+} q^2 \cdot \frac{1}{p_1} g \cdot (q; q^0; x) \frac{1}{p_2^1}, \cdot (p_2; q^0) \\
& + \frac{1}{2} \frac{x}{0} \frac{Z_1}{q^2 dq q^0 dq^0} \frac{Z_1}{dx} \cdot (p_1; q) \frac{\sim^2}{4M_N} \frac{p_1^2}{p_1^2} + \frac{8+}{4} q^2 \cdot \frac{1}{p_1} g \cdot (q; q^0; x) \frac{1}{p_2^1}, \cdot (p_2; q^0) : \quad (24b)
\end{aligned}$$

The overlap integrals are obtained by setting $H_0 = 0$. Furthermore, h_{ji} is given by

$$\begin{aligned}
h \cdot j \cdot j \cdot i = & \int_0^x p^2 dp q^2 dq \frac{\sim^2}{4M_N} p^2 [(p;q)]^2 \\
& + \int_0^x q^2 dq q^0 dq^0 \int_1^1 dx (p_1;q) \frac{\sim^2}{2M_N} p_1^2 \frac{1}{p_1} g (q;q^0;x) \frac{1}{p_2} , (p_2;q^0) \\
& ; \\
& + \int_0^x p^2 dp q^2 dq (p;q) \frac{\sim^2}{8M_N} p^2 + \frac{8+}{4+} q^2 ; + \frac{2(8+)}{4+} pqf ; + (p;q) \\
& ; \\
& + \int_0^x q^2 dq q^0 dq^0 \int_1^1 dx (p;q) \frac{\sim^2}{16M_N} q^2 + q^0 2qq^0 x \frac{1}{p_1} g ; (q;q^0;x) \frac{1}{p_2} , (p;q^0) : \quad (25)
\end{aligned}$$

Here, f_0 is given by

$$\begin{aligned}
f_0 &= \frac{d\mathbf{p}_2 d\mathbf{q}_2 h \mathbf{p}_2 \mathbf{q}_2 i(\mathbf{p}_2 \mathbf{q}_2) \mathbf{h} \mathbf{p}_2 \mathbf{q}_2 j^0 i}{(1)^{1+1^0+L} \mathbf{b}_1 \mathbf{b}_2 h^1 010 j^1 i h^2 010 j^2 i^0} \quad (\text{LS coupling}); \\
&= (1)^{1+1^0+L} \mathbf{b}_1 \mathbf{b}_2 h^1 010 j^1 i h^2 010 j^2 i^0 \quad (\text{LS coupling}); \\
&= (1)^{1+1^0+1+1^0} \mathbf{b}_1 \mathbf{b}_2 \mathbf{p} \mathbf{h} \mathbf{p}^0 h^1 010 j^1 i h^2 010 j^2 i^0 \quad (\text{X coupling}); \\
&\quad \times (1)^L (\mathbf{b})^2 \mathbf{J}^L \mathbf{L}^{\frac{1}{2}} \mathbf{J}^0 \mathbf{L}^{\frac{1}{2}} \mathbf{J}^0 \mathbf{L}^{\frac{1}{2}} \mathbf{J}^0 \mathbf{L}^{\frac{1}{2}} \quad (\mathbf{jj} \text{ coupling}); \quad (26)
\end{aligned}$$

C. Transfer matrix and effective N potentials

The $T-m$ atrix is obtained by solving the partial-wave Lippmann-Schwinger equation

$$T(p; p^0; E) = V(p; p^0) - \frac{4}{(2\pi)^3} \frac{2}{\omega^2} \int_0^{Z_1} k^2 dk V(k; k) \frac{1}{\omega^2 + k^2} T(k; p^0; E); \quad (27)$$

where $\gamma = \frac{1}{4} = (4 + \dots) \mathbb{M}_N$ is the reduced mass and $E = \sqrt{(\gamma^2 - 2 \dots)^2}$ is a negative energy. The partial-wave component $V(p; p^0)$ for the Born kernel $V(p; p^0)$ is

defined through

$$V(p; p^0) = 4 \sum_{\lambda} V_{\lambda}(p; p^0) \sum_m Y_m(p) Y_m(p^0); \quad (28)$$

and the $\langle \bar{p} | T(E) | p^0 \rangle$ in Eq. (11b) is given by $T(p; p^0; E)$ with an extra factor $4 = (2)^3$.

For the effective N potential, we assume a Minnesota-type central force [43].

$$v_N = v^1(E) \frac{1-P}{2} + v^3(E) \frac{1+P}{2} - \frac{u}{2} + \frac{2-u}{2} P_r \quad ; \quad (29)$$

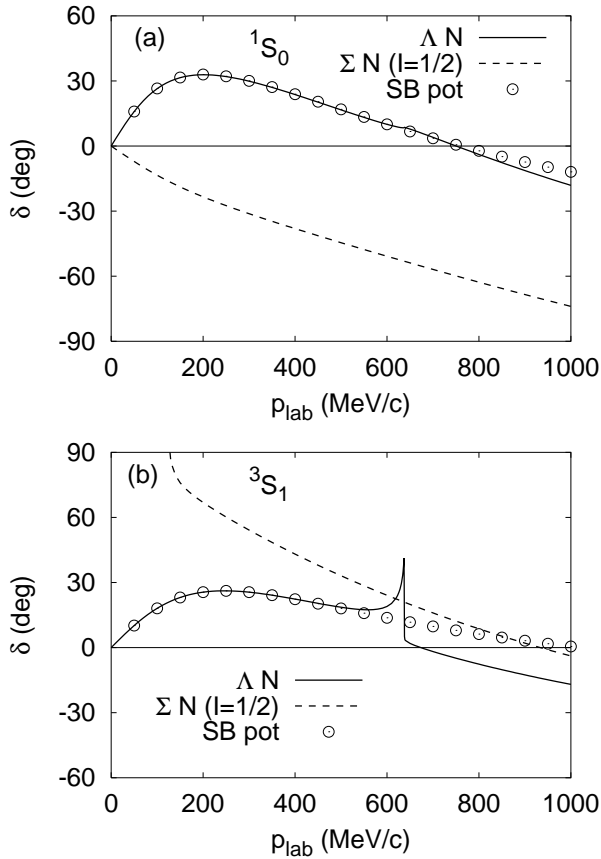


FIG. 1: N - N 1S_0 (a) and 3S_1 (b) phase shifts for the isospin $I = 1/2$ channel, calculated with fss2 [44] (solid and dashed curves) and with the SB potential (circles).

where $v(^1E)$ and $v(^3E)$ are simple two-range Gaussian potentials generated from the 1S_0 and 3S_1 phase shifts predicted by the quark-m odel N interaction, fss2. We use the inversion m ethod based on supersym m etric quantum m echanics, developed in Ref. [41], to derive phase shift equivalent local potentials. These potentials are then tted by two-range Gaussian functions. These are given by

$$\begin{aligned} v(^1S_0) &= 128.0 \exp(-0.8908 r^2) \\ &\quad + 1015 \exp(-5.383 r^2); \\ v(^3S_1) &= 56.31 \exp(-0.7517 r^2) \\ &\quad + 1072 \exp(-13.74 r^2); \end{aligned} \quad (30)$$

where r is the relative distance between and N . In the following, we call this effective N potential the SB potential. Figure 1 shows that these potentials t the low-energy behavior of the 1S_0 and 3S_1 N phase shifts obtained by the full N - N coupled-channel RGM calculations of fss2. In the 3S_1 state, only the low-energy region is tted, since the cusp region cannot be tted in a single-channel calculation. This potential overestimates the 3S_1 phase shift in the higher energy region. The procedure to calculate the B orn kernel for the simple

$(0s)^4$ -cluster wave function is discussed in Appendix B. Here we only give the nal result for the partial-wave components:

$$V^i(q_F; q_i) = \sum_{i=1}^{X^4} X_d^i V^d(q_F; q_i; i) + X_e^i V^e(q_F; q_i; i); \quad (31)$$

Here, X_d^i and X_e^i are spin-isospin factors de ned in Eq. (B12) and tabulated in Table II for the present two-range Gaussian potentials. The explicit functional form of $V^d(q_F; q_i; i)$ and $V^e(q_F; q_i; i)$ are given in Eq. (B13).

In this paper, we also examine the N e ective forces [33] used by H iyama et al. [7] for comparison. These potentials are generated from the G-m atrix calculations of various O BEP potentials. They are parameterized as

$$\begin{aligned} V_N &= \sum_{i=1}^{X^3} h v_0^{(i)}_{\text{even}} + v^{(i)}_{\text{even}} \left(\begin{array}{cc} 1 & 2 \end{array} \right) \frac{i(1+P_r)}{2} \\ &\quad + h v_0^{(i)}_{\text{odd}} + v^{(i)}_{\text{odd}} \left(\begin{array}{cc} 1 & 2 \end{array} \right) \frac{i(1-P_r)}{2} e^{(r-i)^2}; \end{aligned} \quad (32)$$

Since the spin-spin term does not contribute to the spin saturated -cluster, the spin-isospin factors in Eq. (31) (with $i \neq 1 = (i)^2$, $i = 1-3$) are given by

$$\begin{aligned} X_d^i &= 2 v_0^{(i)}_{\text{even}} + v_0^{(i)}_{\text{odd}}; \\ X_e^i &= 2 v_0^{(i)}_{\text{even}} - v_0^{(i)}_{\text{odd}}; \end{aligned} \quad (33)$$

The explicit values for $v_0^{(i)}_{\text{even}}$ and $v_0^{(i)}_{\text{odd}}$ ($i = 1-3$) generated from N ijm egen m odels, NS, ND, NF, and J ulich potentials, JA, JB, are given in Ref. [7]. Table V of Ref. [7] includes a m isprint for NS: the width parameters i for this potential are $1.50 - 1.0 - 0.55$, instead of $1.50 - 0.90 - 0.50$ for the other potentials.]

The binding energy of the bound state depends on the h.o. width parameter of the -cluster. Table III shows that the SB potential of Eq. (30) overbinds the ${}^5\text{He}$ energy by more than 1.6 MeV. It also shows that the u-dependence is very weak, which implies that ${}^5\text{He}$ is an S-wave dominated system. It is well known that a central single-channel N e ective force that ts the low-energy N total cross section and the ground-state energies of ${}^3\text{H}$, ${}^4\text{H}$ and ${}^4\text{He}$ always overestimates the ${}^5\text{He}$

TABLE II: spin- avor coe cients for the M innesota-type SB potential with $v = v_0 e^{-r^2}$.

i	X_d	X_e	i
1, 2	$\frac{u}{2} v_0 {}^1S$	1 $\frac{u}{2} v_0 {}^1S$	1S
3, 4	$\frac{3u}{2} v_0 {}^3S$	3 1 $\frac{u}{2} v_0 {}^3S$	3S

TABLE III: Bound-state energies for the system, $E(^5\text{He})$ (in MeV), calculated by the original SB potential with $f = 1$. The h.o. width parameters, $= 0.275 \text{ fm}^2$ and $= 0.257 \text{ fm}^2$ are assumed for the $(0s)^4$ -cluster. The experimental value is $E^{\text{exp}}(^5\text{He}) = 3.12 \pm 0.02 \text{ MeV}$.

u	$= 0.275 \text{ fm}^2$	$= 0.257 \text{ fm}^2$
1	4.975	4.747
0.6	4.946	4.728

binding energy by more than 2 MeV, due to a lack of mixing and tensor force [45{48]. In order to circumvent this difficulty, we introduce a reduction factor, f , in the attractive part of the 3S_1 potential in Eq. (30) and use

$$v(^3S_1) = 56.31 f \exp(-0.7517 r^2) + 1072 \exp(-13.74 r^2); \quad (34)$$

in the following Faddeev calculations. The choice $f = 0.8821$ for $= 0.275 \text{ fm}^2$ and $f = 0.8923$ for $= 0.257 \text{ fm}^2$ reproduces the desired value $E(^5\text{He}) = 3.120 \text{ MeV}$. The bound-state energies predicted by the NS-JB potentials for the effective N interaction deviate from the original fit in Ref. [7] by 110 keV – 170 keV (3.23 – 3.29 MeV). This is because they used a slightly different expression from ours for the exchange term of the potential. For the Faddeev calculations using the Minnesota 3-range force for the RGM kernel ($= 0.257 \text{ fm}^2$), we readjusted the strength of the original NS-JB N potentials in order to fit the precise ^5He energy, 3.120 MeV. This is achieved by slightly (less than 0.36%) modifying the strength of the short-range repulsive term (the third component) of the original G-matrix potentials.

The phase shifts are also calculated, although there is no experimental data available. The S-wave phase shift shows a monotonic decrease from 180°, similar to Fig. 9 of Ref. [36]. In the energy region $E_{\text{cm}}: () = 0 - 20 \text{ MeV}$, the phase shifts of the higher partial waves rapidly decrease, starting from 20 – 30° for the P wave. This implies that the potential is very much of the Yukawa type, and our lack of knowledge of the interaction in higher partial waves may not become a serious problem in the Faddeev calculations.

D. T-matrix and effective NN Potentials

The T-matrix used for the 3 and Faddeev calculations is generated from the RGM kernel which uses an effective NN potential similar to Eq. (29). In the notation used in Ref. [49], the RGM kernel, $V^{\text{RGM}}(") = V_D + V_D^{\text{CL}} + G + G^{\text{CL}} + "K$ consists of the direct potential V_D , the direct Coulomb potential V_D^{CL} , the sum of the exchange kinetic-energy and interaction kernels, $G = G^K + G^V$, the Coulomb exchange

kernel G^{CL} , and the exchange normalization kernel K . The Born kernel of each term is given in Appendix C. We have to eliminate redundant components from the energy-dependent partial wave T-matrix, $T(p;p^0;E;")$, which satisfies the Lippmann-Schwinger equation similar to Eq. (27). This is necessary only for the S-wave ($= 0$) and D-wave ($= 2$) components, for which there exist two and one h.o. Pauli-redundant states, $u_n(p)$, respectively. Here, $u_n(p)$ are essentially the h.o. wave functions in the momentum representation with the total h.o. quanta $N = 2n + = 0$ and 2, satisfying $K u_n = u_n$. They are explicitly given by

$$u_n(p) = (-1)^n \frac{(2)}{4} R_n(p; \frac{1}{4}) \quad (35)$$

with $= 2$, in terms of the standard three-dimensional h.o. radial wave function $R_n(r;)$ in the coordinate representation. The RGM T-matrices defined in Ref. [14] are calculated by

$$\begin{aligned} \mathbb{F}(p;p^0;E;") &= T(p;p^0;E;") \\ &+ \frac{\sim^2}{4M_N} \frac{2 + p^2}{(2 + \sim^2)} \frac{2 + p^{02}}{(2 + \sim^{02})} \begin{cases} \frac{p}{n=0} u_{n0}(p) u_{n0}(p^0) \\ u_{02}(p) u_{02}(p^0) \end{cases} \\ &\text{for } = 0; 2; \end{aligned} \quad (36)$$

where $\sim^2 = (4M_N E = \sim^2)$ and $\sim^2 = (4M_N " = \sim^2)$. For the higher partial waves with $= 4$, we define $\mathbb{F}(p;p^0;E;") = T(p;p^0;E;")$. The RGM T-matrices in Eq. (36) satisfy the orthogonality condition

$$u_n(p) = \frac{4}{(2)^3} \frac{4M_N}{\sim^2} \int_0^{\sim 1} p^{02} dp^0 \mathbb{F}(p;p^0;E;") \frac{u_n(p^0)}{2 + p^{02}}; \quad (37)$$

for $n = 0; 1$ ($= 0$) and $n = 0$ ($= 2$). Owing to this relationship, we can prove the orthogonality of the total wave function Eq. (2) to the Pauli-forbidden states $u_n(p)$.

For the effective NN force, we mainly use the three-range Minnesota (MN) force [43] with the exchange-mixture parameter, $u = 0.94687$, and the h.o. width parameter, $= 0.257 \text{ fm}^2$, for the $(0s)^4$ -clusters. We also use the two-range Volkov No.1 (VN1) and No.2 (VN2) forces [50], in order to compare our 3 results with the microscopic RGM [38, 51] and GCM [39] calculations. The Majorana parameters m of the Volkov forces and the h.o. width parameters are $m = 0.575$ and $= 0.2515 \text{ fm}^2$ for VN1, and $m = 0.59$ and $= 0.275 \text{ fm}^2$ for VN2. The RGM calculations using these effective NN forces and the complete Coulomb kernel reasonably reproduce the empirical phase shifts of the S-, D-, and G-waves, as well as the S-wave resonance near the threshold. However, the best fit to the

experiment is obtained by the three-range MN force. For the VN 2 force, the S-wave resonance appears as a bound state with the binding energy $B = 245$ keV. Although the VN 1 force reproduces this resonance, the overall π to the π phase shifts is less impressive compared to the MN force. In the RGM calculation, the precise determination of the resonance energy is not easy even in the two- system, because of the presence of the Coulomb force. In the present Lippmann-Schwinger formalism in the momentum representation, the method by Vincent and Phatak [52] is used for solving the scattering problem with the full Coulomb force at the nucleon level. We find that the 0^+ resonance energy is 0.18 MeV and 0.14 MeV for VN 1 force and the MN force, respectively. This should be compared with the experimental value 0.092 MeV.

For the Coulomb force in the 3 and Faddeev calculations, we use the cut-off Coulomb force

$$v_{i,j}^{C_L}(r) = \frac{1 + z(i)}{2} \frac{1 + z(j)}{2} \frac{e^2}{r} \quad (R - r); \quad (38)$$

with the cut-off radius R_C , since the full Coulomb force leads to a singularity in the diagonal T-matrix. Here (x) is the Heaviside step function. For the most compact 3 ground state, this approximation with $R_C = 10$ fm is good enough to obtain 1-2 keV accuracy. The Coulomb exchange kernel for Eq. (38) is calculated analytically, which is also given in Appendix C. The partial-wave decomposition of the RGM kernel is carried out numerically using the Gauss-Legendre 20-point quadrature formula, when the Coulomb force is not included. When the cut-off Coulomb force with $R_C = 14$ fm is employed, it is increased to the 30-point quadrature formula to obtain an accuracy within 1 keV for the exchange Coulomb kernel. The direct Coulomb term is separately integrated with enough number of numerical integration points.

III. RESULTS

To solve the Faddeev equation, we discretize the continuous momentum variable $p(q)$ for the Jacobi coordinate vectors, using the Gauss-Legendre n_1 -point (n_2 -point) quadrature formula, for each of the three intervals of $0 - 1$ fm⁻¹, $1 - 3$ fm⁻¹ and $3 - 6$ fm⁻¹. The small contribution from the intermediate integral over p beyond $p_0 = 6$ fm⁻¹ in the T-matrix calculation is also taken into account by using the Gauss-Legendre n_3 -point quadrature formula through the mapping $p = p_0 + \tan f (1 + x) = 4g$. We need $n_1 = 10$ and $n_3 = 5$, so that 35 points are at least necessary to follow up the inner oscillations of the two- bound-state wave function and the necessary T-matrices for solving the Faddeev equation. These n_3 points for $p > 6$ fm⁻¹ are, however, not included for solving the Faddeev equation, since it causes a numerical instability for the interpolation. The momentum region $q = 6$ fm⁻¹ - 1 is also discretized by the n_3 point formula just as in the p discretization. We

take $n_1 \cdot n_2 \cdot n_3 = 15 \cdot 10 \cdot 5$ for the 3 system and $10 \cdot 10 \cdot 5$ for the system, respectively, unless otherwise specified. The modified spline interpolation technique developed in [53] is employed to generate the rearrangement matrices. For the large-scale diagonalization of non-symmetric matrices, the Arnoldi-Lanczos algorithm developed in the ARPACK subroutine package [54] is very useful.

A. 3 Faddeev calculation

In order to make sure that our Faddeev equation is solved correctly, we first carried out the standard 3-particle Faddeev calculation by using the angular-momentum dependent Ali-Bodmer potential of d type (ABd). We find that the 3 energy, $E_3 = 6.423$ MeV without Coulomb force, is consistent with previous calculations [9]. Here, we used $\sim^2 = M = 10.4465$ MeV fm² and $e^2 = 1.44$ MeV fm for comparison. When the cut-off Coulomb force is included, our value 1.527 MeV is 4 keV lower than the 1.523 MeV given in Table 1 of [9]. This difference is due to a slightly different treatment of the Coulomb force between the two calculations. The small 3 binding energy implies that the Ali-Bodmer phenomenological potential cannot describe the ground state of ¹²C with a compact shell-model-like structure.

TABLE IV: Results of 3 Faddeev calculations, using the RGM kernel, with and without the Coulomb effect. The parenthesized numbers indicate the results when the cut-off Coulomb force with $R_C = 10$ fm are included at the nucleon level. Partial waves up to m_{ax} are included in (1) and (2)-channels. The heading " $\langle \rangle_2$ " is the expectation value of the two- Hamiltonian with respect to the 3 bound state solution, E_3 the 3 bound-state energy, and $c_{(04)}$ the overlap between the 3 bound-state wave function and the $SU_3(04)$ shell-model configuration. For the MN force, the result of the variational calculation using the translationally invariant h.o. basis (h.o. var.) is also given for comparison, where h.o. quanta up to $N = 60$ are included.

Force	m_{ax}	$\langle \rangle_2$	E_3	$c_{(04)}$
VN 1	4	9.657 (10.887)	10.751 (5.206)	0.900 (0.879)
	6	9.531 (10.779)	10.926 (5.365)	0.896 (0.875)
	8	9.530 (10.778)	10.927 (5.366)	0.896 (0.875)
VN 2	4	8.583 (9.608)	11.202 (5.781)	0.826 (0.795)
	6	8.449 (9.505)	11.415 (5.967)	0.821 (0.790)
	8	8.447 (9.503)	11.417 (5.969)	0.821 (0.790)
MN	4	12.032 (13.603)	15.616 (9.433)	0.979 (0.973)
	6	11.905 (13.482)	15.777 (9.591)	0.978 (0.971)
	8	11.904 (13.481)	15.779 (9.592)	0.978 (0.971)
h.o. var.	11.903 (13.480)	15.781 (9.594)	0.978 (0.971)	

TABLE V : Comparison of the 3 ground-state energies, predicted by the present model (E_3) and by fully microscopic calculations (E_3^{full}). The experimental value is $E_3^{\text{exp}} = 7.275$ MeV. The present model is the Faddeev calculation using the

RGM kernel, including the cut-off Coulomb force with $R_c = 10$ fm. The heading E^{int} implies the internal energy of the $(0s)^4$ -cluster with the h.o.w. width parameter, E_{tot} the total energy from the RGM [51] for MN and [38] for VN2) or GCM [39] for VN1) calculations, and $E_3^{\text{full}} = E_{\text{tot}} - 3E^{\text{int}}$.

Force	(fm ⁻²)	E^{int}	E_{tot}	E_3^{full}	E_3
VN1	0.2515	27.0	87.9	6.9	5.37
VN2	0.275	27.3	89.4	7.5	5.97
MN	0.257	23.9	83.0	11.4	9.59

On the other hand, the present 3 model interacting via the RGM kernel gives enough binding and a large overlap with the compact shell-model like component. Table IV lists the results of such Faddeev calculations for the ground state of the 3 system with and without the Coulomb force. The RGM kernels are generated from the VN1, VN2, and MN forces. When the Coulomb effect is included, the cut-off Coulomb force with $R_c = 10$ fm is employed. In the last column in Table IV, $C_{(04)}$ implies the overlap amplitude of the 3 bound-state function with the SU_3 (04) shell-model configuration. We find that all three effective NN forces yield binding energies comparable with the experimental value $E_3^{\text{exp}} = 7.275$ MeV, although the result of the MN force is a little too large. The dominant component of these 3 ground states is the SU_3 (04) shell-model configuration.

Table V shows the 3 ground-state energies E_3 , predicted in the present three-cluster Faddeev formalism, compared with those obtained by fully microscopic calculations, E_3^{full} . We find that the present three-cluster equation gives 3 energies which are only 1.5–1.8 MeV higher than those of the fully microscopic 3 RGM or GCM calculations. This implies that the three-cluster exchange effect, which is neglected in our three-cluster formalism, but is present in the fully microscopic three-cluster RGM kernel, is attractive in nature, and is not as large as the repulsive three-body force claimed necessary in the semi-microscopic 3 models [2, 4]. This is mainly because the 3 model space used by these authors does not exclude the 3 Pauli-forbidden components accurately, unlike the one used in the present Faddeev formalism.

In Tables IV and V, we also find that the three-range MN force gives a somewhat large overbinding of 2–4 MeV, if the 3 energy E_3 is measured from the 3 threshold. The decomposition of the 3 energy to the kinetic-energy and potential-energy contributions in Table VI implies that this overbinding is due to the large cancellation between these two contributions. In this re-

TABLE VI: Kinetic-and potential-energy contributions to the three-energy E_3 , calculated from $\hbar\mathbf{H}_0\mathbf{i} = 2(3^{\prime\prime}_2 - E_3)$ and $\hbar\mathbf{V}\mathbf{i} = 3(E_3 - 2^{\prime\prime}_2)$. The shell-model component, $C_{(04)}$, is large if $\hbar\mathbf{H}_0\mathbf{i}$ is large.

Force	$^{\prime\prime}_2$	E_3	$\hbar\mathbf{H}_0\mathbf{i}$	$\hbar\mathbf{V}\mathbf{i}$	$C_{(04)}$
VN1	10.822	5.380	75.691	81.071	0.877
VN2	9.562	5.984	69.338	75.322	0.793
MN	13.573	9.640	100.717	110.357	0.972

spect, it is interesting to note that the clusters with $= 0.257$ fm² (which gives the correct rms radius $r = (3=4)^{1/2}$) = 1.48 fm [55] for the simple $(0s)^4$ -cluster) give less binding in the framework of the orthogonality condition model (OCM) [8]. If the h.o. constant parameter is small, a proper treatment of the exchange kernel seems to be essential in order to obtain a large binding energy of the 3 ground state. This is reasonable since the large overlap of two -clusters implies the importance of nucleon exchange effects.

B. Faddeev calculation

For a detailed description of the bound states in the Faddeev calculation, it is important to make sure that the result is converged with respect to the following three conditions:

- 1) convergence with respect to the momentum discretization points,
- 2) convergence with respect to the extension of partial waves included,
- 3) convergence with respect to the cut-off radius R_c , when the cut-off Coulomb force is included.

Among them, the Coulomb effect is the most difficult, since the T -matrix of the full Coulomb force is divergent at the diagonal part and the strong oscillation in the momentum representation in the cut-off Coulomb case does not lead to the correct answer, unless the numerical angular-momentum projection of the Coulomb kernel (especially the direct Coulomb term) is accurately performed. After all, the Faddeev calculation with the cut-off Coulomb force is a simple approximation to the unsolvable Faddeev equation with the complete Coulomb force. As to the partial waves, we can easily enumerate all possible angular-momentum states of ⁹Be for the $L = 0^+$ ground state with $J = 1=2$ and the $L = 2^+$ excited state with $J = 5=2$ and $3/2$ in the LS coupling scheme. If no spin-orbit force is introduced, the $J = 5=2$ and $3/2$ excited states are degenerate and the LS-coupling scheme is more efficient than the jj-coupling scheme to reduce the number of channels coupled in the calculation. In the following, the angular-

momentum truncation is specified by $\max^{-1_{\max}}$ values for the and pairs. For example, D-P in the ground-state calculation implies a 4-channel calculation and G-G in the $L = 2^+$ calculation a 19-channel calculation. The largest model space adopted is I-I, which is an 11-channel calculation for $L = 0^+$ and a 28-channel calculation for $L = 2^+$. Note that the variational calculation in Ref. [7] uses a rather restricted model space; i.e., a three-channel calculation with $\max = 2$ and $1_{\max} = 0$, although the meaning of angular-momentum truncation is a little different from ours. For the momentum discretization points, we find that the energy change due to the increase of $n_1 \cdot n_2 \cdot n_3$ is very much R_c dependent. It is usually positive if we go from $n_1 \cdot n_2 \cdot n_3 = 5 \cdot 5 \cdot 5$ to $n_1 \cdot n_2 \cdot n_3 = 10 \cdot 10 \cdot 5$ when the Coulomb force is not included, but it turns out negative when $R_c = 10$ fm and 14 fm. This implies that the Faddeev calculation without Coulomb force usually overestimates the binding energy, if the number of momentum discretization points is not large enough. Since the cut-off Coulomb kernels are oscillating, too small a number of momentum discretization points such as in $n_1 \cdot n_2 \cdot n_3 = 5 \cdot 5 \cdot 5$ case is dangerous when R_c is very large like $R_c = 10$ fm and 14 fm. The orthogonality to the Pauli-forbidden states also deteriorates when the number of momentum discretization points is too small. The squared norm of the Pauli-forbidden components containing the total wave function is typically $10^5 - 10^6$ when $n_1 \cdot n_2 \cdot n_3 = 5 \cdot 5 \cdot 5$, but is improved to less than 10^{13} for $n_1 \cdot n_2 \cdot n_3 = 10 \cdot 10 \cdot 5$. In this paper, we will mainly show the results of $n_1 \cdot n_2 \cdot n_3 = 10 \cdot 10 \cdot 5$, since the energy gain by further extension to $n_1 \cdot n_2 \cdot n_3 = 15 \cdot 15 \cdot 5$ is usually less than 1 keV, when the cut-off Coulomb force with $R_c = 10 - 14$ fm is included.

The energy gain of the ground state, E , and that of the self-consistent $"_2$ values by the increase of the maximum angular-momentum values, $\max^{-1_{\max}}$, are shown in Table V II in the cases when we use the MN or VN2 forces for the interaction and the SB force for the interaction. In these calculations the cut-off Coulomb force with $R_c = 6$ fm is employed. If the S-wave calculation is extended to include the D-wave, the energy gain is about 1 M eV for VN2+SB and 1.2 M eV for MN+SB. The energy gain mainly comes from the partial-wave component with $'_1 = '_2 = 1$ of the ^5He channel. The effect of the partial wave $'_1 = '_2 = 2$ is rather small; i.e., about 50 (VN2) - 60 (MN) keV. Needless to say, the exact energy gain largely depends on the character of the N odd force. The ground-state energy is further improved by 7 (VN2) - 5 (MN) keV and 0.03 (VN1) - 0.0 (MN) keV, according to the extension to the G- and I-waves, respectively. On the other hand, $"_2$ is improved by 160 (VN1) - 281 (MN) keV, 5 - 6 keV and 0.5 - 0.6 keV, according to the extension to the D-, G- and I-waves, respectively. In conclusion, partial waves up to the D-wave are sufficient within 10 keV accuracy. If we wish to have a 1 keV accuracy, we need to take into account at least up to the G-wave. This implies that the partial-wave truncation in the Faddeev formalism is very efficient and the result

converges very rapidly, according to the increase of the partial waves taken into account.

Table V III shows the R_c dependence of the two-energy $E(^3\text{Be})$, the self-consistently determined $"_2$, the three-cluster ground-state energy $E(^3\text{Be})$, the separation energy defined by $B(^3\text{Be}) = E(^3\text{Be}) + M E(^3\text{Be})$, and the expectation value of the Hamiltonian, $"$, when the momentum discretization points with $n_1 \cdot n_2 \cdot n_3 = 10 \cdot 10 \cdot 5$ and the partial waves up to I-I are used in the MN plus SB model. The energy increase (and the accumulated one) due to the increase of R_c is also shown with the plus sign in the second (and the third) row. We find that the ground-state energy $E(^3\text{Be})$ increases by 1.621 M eV when we move from $R_c = 0$ to $R_c = 6$ fm, which is larger than 1.127 M eV calculated for the free two- bound state. This seems to be natural, since the two- subsystem is more compact in the ^9Be system. The energy increase in the self-consistently determined $"_2$ values is 1.435 M eV, which is about 200 keV smaller than the energy increase in $E(^3\text{Be})$, but is still larger than in the free two- bound state by about 300 keV. This observation is a good example that our self-consistent procedure of determining $"_2$ is reasonably functioning. It is interesting to note that this large Coulomb effect in the three-body ground state; i.e., about 1.4 times larger than in the two- system, is characteristic for the increase of R_c from 0 to 6 fm. For the range from $R_c = 6$ to 10 fm, just the opposite is true and the energy increase in the three-body ground state (85 keV) is smaller than in the two- system (> 133 keV). This is apparently because the free relative wave function is more widely spread than the correlated relative wave function in the ^9Be ground state. The tendency of $"_2$

TABLE V II: Energy gain for the ground state (E) and that of the self-consistent $"_2$ values ($"_2$) in keV, for the extension of the maximum angular-momentum values, $\max^{-1_{\max}}$. The cut-off Coulomb force with $R_c = 6$ fm is included.

Force		VN2+SB			
		E (keV)		$"_2$ (keV)	
$n_1 \cdot n_2 \cdot n_3$		5-5-5	10-10-5	5-5-5	10-10-5
S-S !	D-P	954	954	165	160
D-P !	D-D	50	50	5	5
D-D !	G-G	7	7	6	6
G-G !	I-I	0.03	0.03	0.6	0.6
Force		MN+SB			
		E (keV)		$"_2$ (keV)	
$n_1 \cdot n_2 \cdot n_3$		5-5-5	10-10-5	5-5-5	10-10-5
S-S !	D-P	1165	1172	287	281
D-P !	D-D	57	58	7	7
D-D !	G-G	6	5	7	6
G-G !	I-I	0.1	0.0	0.5	0.5

falls just into the middle of these two extremes. By using this feature, we can easily estimate the full Coulomb effect in the $E(^3\text{Be})$ ground state. We find that the result with $R_c = 10 \text{ fm}$ is accurate within a 1 keV error both for $E(^3\text{Be})$ and $"_2$. From Table V III, the final result for the MN + SB potentials is

$$\begin{aligned} E(^3\text{Be}) &= 27.35 \quad 34.18 = 6.837 \text{ MeV} ; \\ " &= 19.46 \quad 18.27 = 1.181 \text{ MeV} ; \\ " &= 9.215 \quad 7.954 = 1.261 \text{ MeV} ; \\ c_{(40)} &= 0.695 ; \end{aligned} \quad (39)$$

Here we have shown the kinetic-energy and potential-energy contributions separately in each energy, and $c_{(40)}$ is the overlap amplitude of the ${}^3\text{Be}$ ground-state wave function with the shell-model (40) wave function. [Note that the sum of the $"_2$ potential energy and twice of the $"$ potential energy is the potential energy of $E(^3\text{Be})$, but this is not true for the kinetic-energy term s.] We have also carried out the similar analysis in the VN 2+ SB model. The converged result of the VN 2+ SB forces, including the cut-off Coulomb force with $R_c = 14 \text{ fm}$, is given by

$$\begin{aligned} E(^3\text{Be}) &= 21.21 \quad 28.09 = 6.879 \text{ MeV} ; \\ " &= 13.64 \quad 12.99 = 0.649 \text{ MeV} ; \\ " &= 8.264 \quad 7.548 = 0.715 \text{ MeV} ; \\ c_{(40)} &= 0.569 ; \end{aligned} \quad (40)$$

If we compare this result with Eq. (39) for the MN force, we find that the energy gain by the more attractive VN 2 force is only 42 keV. This result is rather surprising, if we consider that the VN 2 force gives a two- bound state with energy $E_2 = 245 \text{ keV}$. The interaction by the SB force is also more attractive than in the MN force case due to the different choice of the h.o. width parameter. In other words, the ground state energy of ${}^3\text{Be}$ is not much affected by the poor and interactions, as long as we find a well converged value by taking enough partial waves and a large number of momentum discretization points. On the other hand, the $"_2$ and $"$ values for the MN force are larger than those for the VN 2 force by almost 500 keV. This may be related to the difference of values in the two calculations. The smaller value, 0.257 fm^2 , in the MN force calculation means more extended α -clusters than in the VN 2 calculation ($= 0.275 \text{ fm}^2$), which implies in turn that the relative wave functions in the 2⁺ and subsystems should be more compact in the MN case. This can be confirmed by comparing the kinetic-energy contributions in $E(^3\text{Be})$, $"_2$ and $"$ in Eqs. (39) and (40). For example, the kinetic-energy contribution in $"_2$ is 13.64 MeV in the VN 2 case, while in the MN case it has a much larger value 19.46 MeV. The compactness of the relative wave function in the MN case is also reflected in the fact that $c_{(40)}$ is larger in the MN case, even though the binding energy is smaller. Comparing the result in Eq. (39) with the experimental value

TABLE V III: Cut-off radius (R_c) dependence of the Coulomb energies in the two- bound state energy $E(^3\text{Be})$, the two- expectation value $"_2$, the three-body bound state energy $E(^3\text{Be})$, the separation energy $B(^3\text{Be})$, and the expectation value $"$. Calculations are carried out by using $n_1 \cdot n_2 \cdot n_3 = 10 \cdot 10 \cdot 5$ and the partial waves up to I-I. The three-range MN force and the SB force are used with $= 0.257 \text{ fm}^2$ for the h.o. width parameter of the α -clusters. The energy increase (and the accumulated one) due to the increase of R_c is also shown with the plus sign in the second (and third) row. The experimental separation energy is $B^{\text{exp}}(^3\text{Be}) = 6.71 \pm 0.04 \text{ MeV}$. The suffix "ext" stands for extrapolation.

R_c (fm)	0	6	10	14	1
$E(^3\text{Be})$	1.260	0.133	> 0		0.092
		+ 1.127	> + 0.133		
			(> + 1.260)		(+ 1.352)
$"_2$	0.384	1.051	1.180	1.181	(1.181) _{ext}
		+ 1.435	+ 0.129	+ 0.001	
			(+ 1.564)	(+ 1.565)	(+ 1.565) _{ext}
$E(^3\text{Be})$	8.543	6.922	6.837	6.837	(6.837) _{ext}
		+ 1.621	+ 0.085	+ 0.000	
			(+ 1.706)	(+ 1.706)	(+ 1.706) _{ext}
$B(^3\text{Be})$	7.283	6.789	> 6.837		
"	1.390	1.228	1.260	1.261	(+ 1.261) _{ext}

$E^{\text{exp}}(^3\text{Be}) = 6.62 \pm 0.04 \text{ MeV}$, we can conclude that the MN + SB combination overbinds the ${}^3\text{Be}$ ground-state energy by 220 keV. This is partly because our SB potential is of the pure Serber type ($u = 1$). If we choose $u = 0.82$ for the SB force, the combination with the present MN force and $= 0.257 \text{ fm}^2$ yields $E(^3\text{Be}) = 6.621 \text{ MeV}$. In this case, the ${}^5\text{He}$ bound-state energy is 3.105 MeV.

We list the results of various effective forces used by Hyun et al. in Table IX, when they are used in combination with the MN force for the RGM kernel. The calculations are carried out with $n_1 \cdot n_2 \cdot n_3 = 10 \cdot 10 \cdot 5$, $R_c = 10 \text{ fm}$, and the partial waves up to the G-wave, to obtain the converged results with the accuracy of 1–2 keV.

Table X lists Faddeev calculations for the 2⁺ excited state, including the cut-off Coulomb force with $R_c = 14 \text{ fm}$. The momentum discretization points with $n_1 \cdot n_2 \cdot n_3 = 10 \cdot 10 \cdot 5$ are employed. When the partial waves are restricted to D-S plus S-D, the 2⁺-state energy is located above the $+ {}^5\text{He}$ threshold with the threshold energy 3.12 MeV. The listing therefore starts from the 7-channel calculation with D-P. We find that the result is almost converged with I-I and $R_c = 14 \text{ fm}$, within the accuracy of 1 keV. The final result for the 2⁺ excited

TABLE IX : Faddeev calculations for the $L = 0^+$ ground state, including the cut-off Coulomb force with $R_c = 10 \text{ fm}$. The RGM kernel is generated from the three-range MN force with $u = 0.94687$ and $\lambda = 0.257 \text{ fm}^{-2}$ for the h.o. width parameter of the α -clusters. The G-matrix based effective N forces in Ref. [7] are used for the interaction, by slightly modifying the short-range repulsive part to fit the separation energy $E(^9\text{Be}) = 3.120 \text{ MeV}$. Partial waves up to l_{\max} are included in the ^1S channel and those up to l_{\max} are included in the ^3S channel. The heading $E(^9\text{Be})$ is the three-body ground-state energy of ^9Be in the ^1S model, $\langle \langle \rangle \rangle_2$ the two- α expectation value determined self-consistently, and $\langle \rangle$ the α -expectation value, and $C_{(40)}$ is the overlap with the shell model (40) wave function.

force	l_{\max}	$E(^9\text{Be})$	$\langle \langle \rangle \rangle_2$	$\langle \rangle$	$C_{(40)}$
NS	S-S	5.580	0.909	1.136	0.606
	D-P	6.681	1.122	1.250	0.683
	D-D	6.736	1.133	1.255	0.686
ND	G-G	6.743	1.132	1.257	0.686
	S-S	5.734	0.764	0.774	0.579
	D-P	7.375	1.136	0.838	0.693
NF	D-D	7.478	1.159	0.842	0.697
	G-G	7.483	1.157	0.843	0.697
	S-S	5.682	0.802	0.882	0.587
JA	D-P	6.839	1.009	0.942	0.666
	D-D	6.901	1.021	0.944	0.669
	G-G	6.906	1.020	0.944	0.669
JB	S-S	5.620	0.862	1.030	0.599
	D-P	6.622	1.022	1.112	0.667
	D-D	6.672	1.031	1.114	0.669
JB	G-G	6.677	1.031	1.115	0.669
	S-S	5.566	0.915	1.154	0.606
	D-P	6.431	1.027	1.253	0.664
JB	D-D	6.469	1.034	1.255	0.666
	G-G	6.475	1.033	1.256	0.666

state in the MN + SB model is

$$\begin{aligned}
 E &= 29.45 - 33.37 = -3.921 \text{ MeV} ; \\
 \langle \langle \rangle \rangle_2 &= 21.54 - 17.53 = 4.011 \text{ MeV} ; \\
 \langle \rangle &= 9.476 - 7.925 = 1.552 \text{ MeV} ; \\
 C_{(40)} &= 0.645 ;
 \end{aligned} \tag{41}$$

If we compare Eqs. (39) and (41), we find that the 3 MeV excitation energy of the 2^+ state mainly comes from an increase of the two- α kinetic energy (2 MeV) and from the two- α potential energy (1 MeV). This clearly shows the rotational nature of the ground 0^+ and excited 2^+ states, composed of a two- α structure with a weakly coupled .

Table X summarizes the present results with the MN force for the RGM kernel. The SB result shows the overbinding of the ^9Be ground-state energy by about 220

TABLE X : Same as Table IX, but for the $L = 2^+$ excited state with $R_c = 14 \text{ fm}$.

force	l_{\max}	$E(^9\text{Be})$	$\langle \langle \rangle \rangle_2$	$\langle \rangle$	$C_{(40)}$
SB	D-P	3.792	3.984	1.528	0.642
	D-D	3.869	4.011	1.537	0.645
	G-G	3.921	4.010	1.551	0.645
	I-I	3.921	4.011	1.552	0.645
NS	D-P	3.696	3.918	1.519	0.639
	D-D	3.767	3.944	1.526	0.641
	G-G	3.826	3.940	1.544	0.641
	I-I	3.826	3.940	1.545	0.641
ND	D-P	4.372	4.025	1.131	0.648
	D-D	4.513	4.069	1.135	0.651
	G-G	4.548	4.064	1.138	0.651
	I-I	4.548	4.064	1.139	0.651
NF	D-P	3.849	3.823	1.223	0.637
	D-D	3.934	3.849	1.227	0.639
	G-G	3.976	3.847	1.237	0.639
	I-I	3.976	3.847	1.237	0.639
JA	D-P	3.640	3.803	1.381	0.635
	D-D	3.706	3.825	1.385	0.637
	G-G	3.757	3.823	1.402	0.637
	I-I	3.757	3.824	1.402	0.637
JB	D-P	3.456	3.772	1.507	0.632
	D-D	3.505	3.790	1.512	0.633
	G-G	3.564	3.791	1.536	0.634
	I-I	3.564	3.792	1.536	0.634

keV and too small excitation energy of the 2^+ excited state by about 130 keV. Table X also shows a comparison with the results by Hyam et al. [7] for the G-matrix based effective N forces. We find that their results are a little lower than our results by about 70–90 keV. Since their calculation is a variational calculation using a smaller model space than ours, this is not a convergence problem of the variational calculation. A possible reason is the difference between OCM and RGM in the part. They used OCM, while ours is RGM. The OCM usually gives more attractive results than the RGM. In fact, it is well known that 3 OCM usually gives a larger binding energy than the 3 RGM for the ground state of the 3 system [56]. A small difference in the exchange term of the folding potential may also contribute to this difference.

If we arrange the effective N forces in Table XI in the order of more attractive nature, we find

$$\begin{aligned}
 \text{ND} & (7.483) > \text{NF} (6.906) > \text{SB} (6.837) \\
 & > \text{NS} (6.742) > \text{JA} (6.677) > \text{JB} (6.474) ;
 \end{aligned} \tag{42}$$

TABLE X I: Summary of the ground-state energy $E_{\text{gr}}(0^+)$ and the 2^+ excitation energy $E_x(2^+)$ in MeV, calculated by solving the Faddeev equation for the system in the LS coupling scheme. The RGM kernel is generated from the three-range MN force with $u = 0.94687$ and $\gamma = 0.257 \text{ fm}^{-2}$ for the h.o.w width parameter of the α -clusters.

V_N	$E_{\text{gr}}(0^+)$ (MeV)		$E_x(2^+)$ (MeV)	
	present	Ref. [7]		
SB	6.837		2.915	
NS	6.742	6.81	2.916	
ND	7.483	7.57	2.935	
NF	6.906	7.00	2.930	
JA	6.677	6.76	2.919	
JB	6.474	6.55	2.911	
Exp't	6.62	0.04	3.029 (3)	
			3.060 (3)	

The experimental value 6.62 0.04 MeV is located between JA and JB. However, this does not mean that the Jülich potentials JA and JB are the most correct N interactions. It is well known that the spin-spin central term of these Jülich potentials are completely wrong and that they fail to reproduce the observed energy spectrum of the ${}^4\text{H}$ and ${}^4\text{He}$ systems [57]. As for the 2^+ excitation energy, all the results in Table X I are between 2.91–2.94 MeV. They are too small by 110–130 keV with respect to the average value 3.04 MeV of the two resonances recently observed by γ -ray spectroscopy [31]. Since the experimental error bars are at most 40 keV even in the $(\text{K}^+ + \text{K}^-)$ reaction [27], this is a meaningful disagreement. It would be interesting to examine the 's splitting of the $5=2^+ - 3=2^+$ states, by introducing a small N spin-orbit force predicted by our quark-model interaction.

In order to show that the present RGM kernel gives a better result than simple potentials, we show in Table X II some results of Faddeev calculations using the Ali-Bodmer potential, ABd [12], and the Buck, Friedrich, and W heatley potential, BFW [11]. In these cases, there is no need for a self-consistent procedure to determine 2 . We only use the SB potential for the interaction, since results with other effective N forces are essentially evaluated from the above discussion in the case of the RGM kernel. In these particle models, we customarily use $\gamma^2 = M_N = 10.4465 \text{ MeV fm}^2$ and $e^2 = 1.44 \text{ MeV fm}$. The momentum discretization points with $n_1=n_2=n_3=15-10-5$ are employed. For the Coulomb potential, the folding potential of the cut-off Coulomb force with the $(0s)^4$ shell model wave function is used with $R_C = 10 \text{ fm}$. The h.o.w width parameter of the $(0s)^4$ α -cluster for this Gaussian folding is $\gamma = 0.27127 \text{ fm}^{-2}$ in the ABd case and $\gamma = 0.257 \text{ fm}^{-2}$ in the BFW case. In the ABd case, this value corresponds to the Coulomb-force parameter $\gamma = 3/(2 \cdot 1.44) = 0.601407 \text{ fm}^{-1}$

TABLE X II: Faddeev calculations for the $L = 0^+$ ground state by the Ali-Bodmer (ABd) [12] and Buck, Friedrich, and W heatley (BFW) [11] potentials. The SB N force is used for the interaction. The cut-off Coulomb force is included at the nucleon level with with $R_C = 10 \text{ fm}$. The h.o.w width parameters of the α -clusters are assumed to be $\gamma = 0.27127 \text{ fm}^{-2}$ (ABd) and $\gamma = 0.257 \text{ fm}^{-2}$ (BFW). The parameters $\gamma^2 = M_N = 10.4465 \text{ MeV fm}^2$ and $e^2 = 1.44 \text{ MeV fm}$ are used. Partial waves up to 2 are included in the α -channel and those up to ${}^1_{\text{max}}$ in the α -channel. The momentum discretization points with $n_1=n_2=n_3=15-10-5$ are employed. The bound-state energy $E({}^5\text{He})$ for the SB N force is given in the first column.

ABd + SB					
$E({}^5\text{He})$	2	$E({}^9\text{Be})$	2	0	$c_{(40)}$
3.183	S-S	6.409	0.970	0.503	0.466
	D-P	7.091	1.013	0.532	0.497
	D-D	7.147	1.013	0.526	0.499
	G-G	7.153	1.018	0.518	0.498
	I-I	7.153	1.018	0.517	0.498
BFW + SB					
$E({}^5\text{He})$	2	$E({}^9\text{Be})$	2	0	$c_{(40)}$
3.066	S-S	5.544	0.861	1.776	0.630
	D-P	6.971	1.147	1.973	0.724
	D-D	7.038	1.155	1.979	0.728
	G-G	7.043	1.161	1.980	0.728
	I-I	7.043	1.161	1.980	0.728

and the rms radius $r = 1.44 \text{ fm}$. Since this value is also used for the α -cluster folding for the N potential, the bound-state energy $E({}^5\text{He})$ is a little shifted from the fitted experimental value 3.12 MeV. [The different $\gamma^2 = M_N$ value also affects this difference.] Since the energy change is only about 0.06 MeV, we do not readjust the potential parameters of the N force. In the BFW case, the value, 0.257 fm^{-2} , corresponds to $\gamma = 3/(2 \cdot 1.44) = 0.58538 \text{ fm}^{-1}$ and the rms radius of the α -cluster is $r = 3/(2 \cdot 1.44) = 1.48 \text{ fm}$. In this case the difference of the N bound-state energy, 0.054 MeV, from 3.12 MeV is solely from the different $\gamma^2 = M_N$ value. The bound-state solutions of the BFW potential are used for the pairwise Pauli-forbidden states. The elimination of the Pauli-forbidden components from the three-body total wave function is always inspected by calculating their squared norm, which is of the order of 10^{-13} .

We find that the ground-state energy by the ABd potential is lower than the result of the MN force in Eq. (39) by 0.3 MeV. Note that even in this case the energy gain by the higher partial waves than the S wave is appreciable, i.e., 0.7 MeV. This implies that the S-wave assumption adopted by Filikhin and Gal [34] is not valid. They used a little different version of the Ali-Bodmer potential (type (a) with 125 MeV modified by 120 MeV) and obtained $E({}^9\text{Be}) = 6.55 \text{ MeV}$ in the S-wave ap-

proximation. We expect an energy gain of about 0.7 MeV from the higher partial waves and their result is overbound, in comparison with the experimental value, 6.62 0.04 MeV. In Table X II, we find that the BFW potential gives a better result than the Al-Bodmer force, but the energy is still lower than in the MN force case by 0.2 MeV. In this case we find that the effect of partial waves higher than the S wave is quite appreciable, i.e.,

1.5 MeV. This is of course due to the inner oscillation of the relative wave function between the two α -clusters in the ground state. The shell-model like (40) components are about 0.7 in amplitude, which is appreciably larger than $c_{(40)} = 0.5$ in the Al-Bodmer case.

IV. SUMMARY

The three-cluster Faddeev formalism using two-cluster resonating-group method (RGM) kernels opens a way to solve few-baryon systems interacting via quark-model baryon-baryon interactions without spoiling essential features of the RGM kernel; i.e., the non-locality, the energy dependence proportional to the exchange normalization kernel, and the existence of pairwise Pauli-forbidden states in some specific channels. In this paper, we have applied this formalism to three-cluster systems involving α -clusters; i.e., the 3 and α systems. These systems involve all of the above three features for the microscopic interactions between composite particles. In particular, the interaction is a prototype of composite-particle interactions, in which the fully microscopic RGM calculation is easy and very successful. It, however, involves a somewhat complex kernel structure composed of three non-trivial Pauli-forbidden states, and the energy-dependence of the interaction is rather strong in the Pauli-allowed model space. In the present Faddeev formulation, the Pauli-forbidden components between pairwise clusters are completely eliminated from the total wave function of the three clusters. This can be achieved by introducing a special type of RGM \mathbb{F} -matrix calculated from the two-cluster RGM kernel, which satisfies the \mathbb{T} -matrix version of the orthogonality conditions to the relative motion between two clusters. The on-shell and half-on-shell properties of the \mathbb{F} -matrix are just the same as those of the ordinary \mathbb{T} -matrix. This RGM \mathbb{F} -matrix involves a relative energy of two clusters as a parameter, which is determined self-consistently by calculating the expectation value of the two-cluster Hamiltonian with respect to the total wave function resulting from the Faddeev equation. The Faddeev equation using \mathbb{F} -matrices is equivalent to the pairwise orthogonality condition model (OCM) of three-cluster systems, interacting via two-cluster RGM kernels. A nice point of this formalism is that the underlying nucleon-nucleon (NN) and hyperon-nucleon (YN) interactions are more directly related to the structure of three-cluster systems than in the models assuming simple two-cluster potentials.

We have first applied the present formalism to the

ground state of the 3 system by using three different types of effective NN forces, the two-range Volkov forces, No.1 (VN1) and No.2 (VN2), and the three-range Minnesota (MN) force. The three-range MN force reproduces the S-, D- and G-wave phase shifts quite well in the simple $(0s)^4$ model of the clusters. The comparison with the 3 RGM calculation has shown that the present three-cluster formalism using only the RGM kernel gives a good approximation to the microscopic 3 model. The difference of the ground-state energies predicted by these two models is less than 2 MeV. The effect of the antisymmetrization among three α -clusters, which is neglected in our formulation, is attractive and is not so large, as long as the Pauli-allowed model space of the 3 system is properly treated. It is also shown that the three-range MN force gives a lower ground-state energy than the two-range VN1 and VN2 forces, resulting in a somewhat large overbinding of 2–4 MeV of the 3 ground state, if the 3 energy is measured from the 3 threshold.

The application to the ^9Be system has proved that our three-cluster formalism is soundly extended to the systems with two identical clusters, in addition to the systems of three identical clusters like the 3 system and the triton system. Here we have introduced a new effective N force, called the SB force, which is made from the quark-model predictions of the N phase shifts by using an inversion method based on supersymmetric quantum mechanics [41]. The SB force consists of two simple two-range Gaussian potentials which reproduce the low-energy behavior of the 1S_0 and 3S_1 N phase shifts predicted by N–N coupled-channel RGM calculations using the model fss2 [44]. Since any central and single-channel effective N force leads to the well-known overbinding problem of ^5He by about 2 MeV [48], the attractive part of the 3S_1 N potential is reduced by about 10% to reproduce the empirical α -separation energy $B^{\text{exp}}(^5\text{He}) = 3.12 \pm 0.02$ MeV. The odd-state N force is assumed to be zero (pure Serber type). In addition to this SB force, we have also used the effective N forces in Ref. [7] for comparison. The interactions are generated from these N effective forces by the folding procedure with respect to the $(0s)^4$ α -wave function of the clusters.

In the Faddeev calculation, enough partial waves up to $M_{\text{max}} = l_{\text{max}} = 6$ are included both in the and pairs since the relative wave functions between two α -clusters are oscillating at least in the relative S- and D-waves. The detailed analysis shows that the partial waves up to the D-wave are sufficient if we do not mind a 10 keV inaccuracy. If we wish to obtain a 1 keV accuracy, we need to take into account at least up to the G-wave. This implied that the partial-wave truncation is very efficient even in the present Faddeev formalism. The energy gain due to partial waves higher than the S-wave is about 1 MeV for the VN2 force and 1.2 MeV for the MN force, when these interactions are used in combination with the SB force for the interaction. The

Coulomb effect between the two α -clusters is included by a cut-off Coulomb force at the nucleon level. The cut-off radius, $R_c = 10 - 14$ fm seems to be sufficient for a 1 - 2 keV accuracy. In the present formalism, the structure change of two α -clusters inside ^9Be is clearly identified by calculating the kinetic-energy contribution in the two- α expectation value $\langle \alpha \rangle$. The comparison of the Coulomb contributions in the α -bound state, $\langle \alpha \rangle$ and the ^9Be ground state with respect to the change of R_c is very useful to measure the compactness of the two- α configurations in various environments. It is confirmed that the 0^+ ground state and the 2^+ excited state of ^9Be are well described by the contracted two- α cluster structure with a weakly coupled α -particle in the dominant S-wave component. In the present calculation using only central forces, the three-range NN force and the SB potential with the pure-Serber character can reproduce the ground-state and excitation energies of ^9Be within an accuracy of 100 - 200 keV. The results in Ref. [7] based on the OCM framework are also confirmed within 100 keV accuracy. On the other hand, the simple α -particle model using the Alibademer potential, ABD [12], and the OCM using the deep Buck, Friedrich, and Wheatley potential, BFW [11], with bound-state Pauli-forbidden states give an overbinding of the ^9Be ground state by 530 keV and 420 keV, respectively, when the SB force is used for the interaction. Although these energies are rather similar, the effect of partial waves higher than the S-wave is very different; i.e., 0.7 MeV in the Alibademer case and 1.5 MeV in the BFW case. It is natural that the interactions which yield an oscillatory behavior of the relative wave functions, like our RGM kernel and the BFW potential, need more partial waves with a larger energy gain.

There are still many problems left for the future studies. First of all, the readjustment of the 3S attractive part of the SB NN potential is unsatisfactory from the viewpoint of using the fundamental baryon-baryon interactions. The Brueckner rearrangement effect in ^5He is fairly large even for the rather stable α -cluster [48]. In this sense, there is still no consistent description of the s-shell and p-shell hypernuclei even at the level of using effective baryon-baryon interactions. A microscopic description of the interaction may need a more detailed analysis based on the G-matrix theory, for which the folding formula given in Appendix C is very useful. In order to describe the ^9Be excited states realistically, we need to introduce the spin-orbit force and solve the Faddeev equation in the jj-coupling scheme. The recent x-ray spectroscopy experiment [31] indicates a very small spin-orbit splitting for the possible $5=2^+$ and $3=2^+$ resonances. It is interesting to examine the LS components of the quark-model NN interaction, in which the antisymmetric LS interaction ($LS^{(1)}$) is by about a factor two larger than in the Nijmegen models. We expect a large cancellation of the ordinary LS interaction by this $LS^{(1)}$ interaction. An interesting application of the present Faddeev formalism and the T-matrix derived in this study is

to the recent Nagara event [58] for ^6He . For the interaction, we can use the coupled-channel α -N-T-matrix of the quark-m model interaction, fss2. A preliminary result shows that fss2 is at present the only model which can reproduce an appropriate strength of the interaction, $B^{\text{exp}} = 1.01 \pm 0.20$ MeV, deduced from the Nagara event. In a separate paper [22], we will also report another application of the present three-cluster Faddeev formalism to the hypertriton system, in which the quark-m model NN and YY interactions are explicitly used in the NN and NN coupled-channel Faddeev formalism. In this system, a complete Pauli-forbidden state at the quark level exists in the NN subsystem.

Acknowledgments

This work was supported by Grants-in-Aid for Scientific Research (C) from the Japan Society for the Promotion of Science (JSPS) (Nos. 15540270, 15540284, and 15540292). Y. Fujiwara wishes to thank the FNRS foundation of Belgium for making his visit to the Free University of Brussels possible during the summer, 2002.

APPENDIX A: REARRANGEMENT FACTORS OF THREE-CLUSTER SYSTEMS AND THE PARTIAL WAVE DECOMPOSITION

In this appendix, we discuss the procedure to derive the rearrangement factors of three-cluster systems with two identical particles or clusters, by using the Dirac notation. When using the Dirac notation, it is important to fix a coordinate system of the representation. We choose the standard system of the Jacobi coordinates with $\gamma = 3$, and introduce the Jacobi coordinates in the momentum space, $p = p_3$ and $q = q_3$. The other Jacobi coordinates p_1, q_1 , etc. are similarly defined. For an arbitrary function $(p; q; 123)$ in $\gamma = 3$, the effect of the cyclic permutation $P_{(123)}$ of the symmetric group S_3 is

$$\begin{aligned} P_{(123)}(p_2; q_2; 123) &= P_{(123)}^2(p_1; q_1; 231) \\ &= (p_3; q_3; 123); \end{aligned} \quad (\text{A}1)$$

where 123 in $(p; q; 123)$ stands for the spin-isospin variables. For the transposition $P_{(12)}$, Eq. (1) yields

$$\begin{aligned} P_{(12)}(p_3; q_3; 123) &= (p_3; q_3; 213); \\ P_{(12)}(p_1; q_1; 231) &= (p_2; q_2; 132); \\ P_{(12)}(p_2; q_2; 312) &= (p_1; q_1; 321); \end{aligned} \quad (\text{A}2)$$

Note that the momentum sum in p , q , and the sign of p , etc., are uniquely specified by the sequence of 123. For example, $p_2; q_2; 123$ in Eq. (8) actually implies $p_2; q_2; 312$ i.e. In the following, we always use an abbreviated notation, $= (p_3; q_3; 123)$, in the standard coordinate system $\gamma = 3$. The total wave function,

$(q_3; q_3; 123)$, in Eq. (2) is compactly expressed as

$$\begin{aligned} &= P_{(12)} + \\ &= P_{(12)} P_{(123)}^2 + P_{(123)}^2; \end{aligned} \quad (\text{A } 3)$$

where

$$\begin{aligned} (p_3; q_3; 123) &= P_{(123)}^2, (p_3; q_3; 123) \\ &= ' (p_2; q_2; 312); \\ (p_3; q_3; 123) &= P_{(12)} P_{(123)}^2, (p_3; q_3; 123) \\ &= ' (p_1; q_1; 321); \end{aligned} \quad (\text{A } 4)$$

from Eqs. (A 1) and (A 2). If we write the Faddeev equation in terms of and ', it reads

$$\begin{aligned} &= G_0 T_{12} 1 P_{(12)}; \\ &= G_0 T_{13} P_{(12)}'; \end{aligned} \quad (\text{A } 5)$$

In Eq. (3), the Faddeev equation for and ' is given with the notation of the T-matrices, $\mathbf{T} = T_{12}$ and $\mathbf{T} = P_{(123)} T_{13} P_{(123)}^{-1}$, as

$$\begin{aligned} &= G_0 \mathbf{T} 1 P_{(12)} P_{(123)}^2; \\ &= G_0 \mathbf{T} P_{(123)} P_{(23)}'; \end{aligned} \quad (\text{A } 6)$$

Next we calculate the rearrangement factors by taking $h \mathbf{P}_{(123)}^2$ as an example. From the definition of $P_{(123)}$, we find

$$\begin{aligned} h p_3; q_3; 123 \mathbf{P}_{(123)}^2, i &= P_{(123)}^2, (p_3; q_3; 123) \\ &= ' (p_2; q_2; 312) = d p^0 d q^0 (p^0 p_2) (q^0 q_2) \\ &= P_{(123)}^2, (p^0 q^0; 123); \end{aligned} \quad (\text{A } 7)$$

where $P_{(123)}^2$ operates only on the spin-isospin variables of $(p^0 q^0; 123)$. We write $p_3; q_3$ as $p; q$, and make the partial wave decomposition through

$$\begin{aligned} h p; q; 123 \mathbf{P}_{(123)}^2, i &= \sum_{\substack{X \\ h p; q; 123}} h p; q; 123 j i h p; q; \mathbf{P}_{(123)}^2, i; \\ (p^0 q^0; 123) &= \sum_{\substack{X \\ h p^0 q^0; 123}} h p^0 q^0; 123 j i' (p^0 q^0); \end{aligned} \quad (\text{A } 8)$$

Here, the summations are over all the angular-momentum (and also spin, isospin) quantum numbers in the or channel. Then we find

$$h p; q; \mathbf{P}_{(123)}^2, i = \sum_{\substack{X \\ 0}} \sum_{\substack{Z \\ 1}} p^0 d p^0 \sum_{\substack{Z \\ 0}} \sum_{\substack{1}} q^0 d q^0 h p; q; \mathbf{P}_{(123)}^2 p^0 q^0; i_3 2' (p^0 q^0); \quad (\text{A } 9a)$$

$$h p; q; \mathbf{P}_{(123)}^2 p^0 q^0; i_3 2 = \sum_{\substack{X \\ 123}} d p d q d p^0 d q^0 h p; q; 123 i (p^0 p_2) (q^0 q_2) P_{(123)}^2 h p^0 q^0; 123 j i; \quad (\text{A } 9b)$$

Here, p_2 and q_2 are obtained from Eq. (4) by setting $= 2$, $= 3$, and $p = p$, $q = q$. This implies Eq. (A 9b) being explicitly given by

$$\begin{aligned} h p; q; \mathbf{P}_{(123)}^2 p^0 q^0; i_3 2 &= \sum_{\substack{X \\ 123}} d p d q d p^0 d q^0 h p; q; 123 i p + q^0 + \frac{m_2}{m_2 + m_1} q \\ p^0 q - \frac{m_3}{m_3 + m_1} q^0 &= P_{(123)}^2 h p^0 q^0; 123 j i; \end{aligned} \quad (\text{A } 10)$$

We define

$$p_1 = q^0 + \frac{m_2}{m_2 + m_1} q; \quad p_2 = q + \frac{m_3}{m_3 + m_1} q^0; \quad (\text{A } 11)$$

and follow the standard procedure [42]. For the spin-angular (and also isospin) functions, we further separate the orbital angular-momentum part through

$$\begin{aligned} h p; q; 123 j i &= \sum_{\substack{X \\ h p; q; 123}} h p; q; j (') LM i h (') LM; 123 j i = \sum_{\substack{X \\ LM}} Y_{(') LM} (p; q) h (') LM; 123 j i; \\ h p^0 q^0; 123 j i &= \sum_{\substack{X \\ LM}} Y_{('1; '2) LM} (p^0; q^0) h ('1; '2) LM; 123 j i; \end{aligned} \quad (\text{A } 12)$$

Then we find

$$h p; q; \mathbf{P}_{(123)}^2 p^0 q^0; i_3 2 = \frac{1}{2} \sum_{-1}^{Z_1} dx \frac{(p - p_1)}{p^{+2}} \frac{(p^0 - p_1^0)}{p^{0+2}} g (q; q^0; x); \quad (\text{A } 13a)$$

$$h(p; q; \mathcal{P}_{(123)}^2, i) = \frac{1}{2} \int_0^{\infty} q^0 dq^0 \int_1^{\infty} dx \frac{(p_1 p_2)}{p_1^2} g(q; q^0; x) \frac{1}{p_2^2}, \quad (p_2; q^0); \quad (A 13b)$$

where

$$p_1 = p \cdot q^0; \frac{m_2}{m_2 + m_1} q; x; \quad p_2 = p \cdot q; \frac{m_3}{m_3 + m_1} q^0; x; \quad (A 14)$$

with $p(q; q^0; x) = \frac{p}{q^2 + q^{02} + 2qq^0x}$. The rearrangement factor $g(q; q^0; x)$ is given by

$$g(q; q^0; x) = \frac{X}{1+} \frac{X}{2} \frac{q^0}{q^0+} \frac{q^0}{q^0+} \frac{m_2}{m_2+m_1} \frac{m_3}{m_3+m_1} \frac{X}{k} (2k+1) g^{1 \frac{0}{1} k} P_k(x); \quad (A 15a)$$

$$g^{1 \frac{0}{1} k} = (-1) \frac{X}{LM} \frac{X}{123} h(j(\cdot)LM; 123i\mathcal{P}_{(123)}^2 h(\cdot_1 \cdot_2)LM; 123j i G^{1 \frac{0}{1} k L}(\cdot; (\cdot_1 \cdot_2)); \quad (A 15b)$$

with the spatial rearrangement factor

$$\begin{aligned} G^{1 \frac{0}{1} k L}(\cdot; (\cdot_1 \cdot_2)) &= G^{0 \frac{0}{1} k L}(\cdot_1 \cdot_2; (\cdot)) = 4 \frac{(2+1)!(2\cdot_1+1)!}{(2\cdot_1+1)!(2\cdot_2+1)!(2\cdot_1^0+1)!(2\cdot_2^0+1)!} \frac{1}{2} \\ &\quad \frac{dq_1 dq_0}{dq_1 dq_0} Y_{(\cdot_1 \cdot_2)}(q^0; q) Y_{LM}(q) P_k(q; q^0) Y_{(\cdot_1 \cdot_2)}(q; q^0) Y_{LM}(q^0) \\ &= \frac{(2+1)!(2\cdot_1+1)!}{(2\cdot_1)!(2\cdot_2)!(2\cdot_1^0)!(2\cdot_2^0)!} \frac{1}{2} \frac{b b_1 b_2}{b_1 b_2} \frac{X}{f; f^0} h_{20} \cdot 0 \cdot f_0 i h_{20}^0 \cdot 20 \cdot f_0^0 i h_{20}^0 \cdot 10 \cdot f_0^0 i h_{20}^0 \cdot 00 \cdot f_0 i \\ &\quad \begin{matrix} f & L & 1 & f^0 & L & 0 \\ 2 & & & 1 & 0 & 2 \\ & & & & 1 & f & k \end{matrix} \quad : \end{aligned} \quad (A 16)$$

Here, $b = \frac{p}{2+1}$ etc. and $\cdot_2 = \cdot_1, \cdot_2^0 = \cdot_1^0, \cdot_1^0$ with $\cdot_1 = 0, \cdot_1^0 = 0, \cdot_1^0 = 0$. For the spin-isospin part of Eq. (A 15b), some angular momentum recouplings yield

$$\begin{aligned} g^{1 \frac{0}{1} k} &= (-1) G^{1 \frac{0}{1} k L}(\cdot_2; (\cdot_1 \cdot_2)) h_{STz}; \quad \mathcal{P}_{(123)}^2 \frac{1}{3} h_{STz}; \quad i_{\text{spin isospin}} \quad (\text{LS coupling}); \\ &= (-1) \frac{X}{LS} \frac{6}{L} \frac{s_1}{S} \frac{I}{J} \frac{1}{J} \frac{s_1^0}{s_2^0} \frac{j_1}{j_2} \frac{7}{5} \frac{6}{4} \frac{1}{2} \frac{s_2^0}{s_2^0} \frac{j_2}{j_2} \frac{7}{5} G^{1 \frac{0}{1} k L}(\cdot; (\cdot_1 \cdot_2)) h_{STz}; \quad \mathcal{P}_{(123)}^2 \frac{1}{3} h_{STz}; \quad i_{\text{spin isospin}} \\ &\quad (jj \text{ coupling}); \end{aligned} \quad (A 17)$$

where the square bracket implies the unitary form of the 9j coefficients and the quantum numbers are specified by

$$\begin{aligned} j \cdot i &= j[(\cdot)LS]Jz; TTz; \quad j \cdot i = j[(\cdot_1 \cdot_2)LS]Jz; TTz; \quad (\text{LS coupling}); \\ j \cdot i &= j[(\cdot_1)I(\cdot_2)J]Jz; TTz; \quad j \cdot i = j[(\cdot_1 s_1^0)j_1 (\cdot_2 s_2^0)j_2]Jz; TTz; \quad (jj \text{ coupling}); \end{aligned} \quad (A 18)$$

Note that the permutation operator $\mathcal{P}_{(123)}^2$ does not change the total spin and isospin values, S and TT_z .

The other types of rearrangement factors are obtained in a similar way. First, the symmetry of the matrix elements yields

$$h(p; q; \mathcal{P}_{(123)} \mathcal{P}^0; q^0; \cdot_2) = h(p^0; q^0; \mathcal{P}_{(123)}^2 \mathcal{P}; q; \cdot_2); \quad (A 19)$$

The rearrangement factor for the matrix element $h' \mathcal{P}_{(23)} \mathcal{P}^0$ needs a little care, since the mass assignment of the three particles is made in the standard Jacobi coordinates $= 3$. We first use $\mathcal{P}_{(23)} = \mathcal{P}_{(123)} \mathcal{P}_{(12)} \mathcal{P}_{(123)}^{-1}$ and write the matrix element as

$$h' \mathcal{P}_{(23)} \mathcal{P}^0 = \int_{123}^X \int_{123}^Z dp_3 dq_3' \langle p_2; q_2; 312 |' (p_1; q_1; 321) : \quad (A 20)$$

The corresponding rearrangement factor in the Dirac notation is given by

$$\begin{aligned} \text{hp};\text{q}; \mathcal{P}_{(123)} \text{p}^0;\text{q}^0; \text{p}^0_{12} = & \frac{x^z}{123} \text{dp} \text{dq} \text{dp}^0 \text{dq}^0 \text{h} \text{p};\text{q};123i \text{p} + \text{q}^0 + \frac{m_1}{m_1 + m_3} \text{q} \\ & \text{p}^0 + \text{q} + \frac{m_2}{m_2 + m_3} \text{q}^0 \mathcal{P}_{(123)} \text{h} \text{p}^0;\text{q}^0;123j^0i; \end{aligned} \quad (\text{A } 21)$$

from which the result in Eqs. (14) and (15) is easily obtained. Note that the rearrangement factor Eq. (A 21) is symmetric with respect to the interchange between $\text{p};\text{q}$ and $\text{p}^0;\text{q}^0$, since $m_1 = m_2$.

APPENDIX B : A USEFUL FORMULA FOR THE BORN KERNEL

The general procedure to calculate Born kernels of the s -shell clusters, developed in Ref. [59], can also be used to calculate the Born kernel

$$\begin{aligned} V(\text{q}_f; \text{q}_i) &= \text{h} e^{i\text{q}_f \cdot \text{r}} \mathcal{P} e^{i\text{q}_i \cdot \text{r}} \\ &= \text{h} e^{i\text{q}_f \cdot \text{r}} \sum_{j=2}^{x^5} v_{1j} \mathcal{P} e^{i\text{q}_i \cdot \text{r}} \quad i; \end{aligned} \quad (\text{B } 1)$$

where h is the internal wave function of the cluster, p is the spin wave function of the particle and v_{1j} is an effective N interaction. The essential part of this method lies in the correct treatment of the cm motion which is handled by the procedure given in Ref. [60]. This method makes it possible to deal with the most general form of the N interaction with non-static effects like the G-matrix N interaction. In this method, $V(\text{q}_f; \text{q}_i)$ in Eq. (B 1) is calculated from an integral form of the GCM kernel through

$$\begin{aligned} V(\text{q}_f; \text{q}_i) &= \text{h} (X_G) e^{i\text{q}_f \cdot \text{r}} \sum_{j=2}^{x^5} v_{1j} \mathcal{P} e^{i\text{q}_i \cdot \text{r}} \quad i \\ &= \frac{1}{2} \frac{3}{2} e^{\frac{1}{4}(\text{q}_f^2 + \text{q}_i^2)} \int d\text{a} d\text{b} e^{i\text{q}_f \cdot \text{a} + i\text{q}_i \cdot \text{b}} \\ &\quad G(\text{a}; \text{b}); \end{aligned} \quad (\text{B } 2)$$

with

$$G(\text{a}; \text{b}) = \frac{G}{2} \frac{3}{2} \int d\text{R} \text{h}(\text{a}) (0) \sum_{j=2}^{x^5} v_{1j} \quad j \quad (\text{R} + \text{b}) \quad (\text{R}) \quad i; \quad (\text{B } 3)$$

Here, $G = (4 +)$, $= 4 = (4 +)$ with $= M M_N$, and (R) and (R) are the h.o. shell model wave functions of and , centered at R , with the width parameters and , respectively. First we calculate spatial integrals for the spatial part u in $v_{1j} = u_{1j} \delta_{1j}$. These four integrals with $j = 2 - 5$ are all equal because of the antisymmetric property of the cluster. We need to calculate spatial integrals for $u = u(\text{x}_1 - \text{x}_2)$ and $u = u(\text{x}_1 - \text{x}_2) \mathcal{P}_r$, which we call the direct term and the exchange term, respectively. It is important to note that the space exchange operator, \mathcal{P}_r , operates only on

the single-particle coordinates x_1 and x_2 , and does not exchange the and N masses. The procedure to interchange these masses M and M_N simultaneously like in Ref. [7] leads to an erroneous expression [see Eq. (A 1) of [7]], which is apparently wrong since the RGM kernel $\text{h}(\text{r} \cdot \text{a}) \sum_{j=2}^5 v_{1j} \text{j}(\text{r} \cdot \text{b})$ should not involve the mass dependence. The correct expression is the one in which one sets $M_N = M$ in their Eq. (A 1) [see Eq. (B 10b) below]. The most general form of the two-body N matrix elements for the translationally invariant u is parameterized as

$$\text{h} \text{p}_1 \text{p}_2 \mathcal{P} \text{p}_1^0 \text{p}_2^0 i = \frac{1}{(2)^3} (\text{P} - \text{P}^0) u(k^0; \text{q}^0; \text{P}); \quad (\text{B } 4)$$

with

$$\begin{aligned} (\text{P} &= \frac{1}{1+} (\text{p}_1 & \text{p}_2) & ; & \text{p}_1 = \frac{1}{1+} \text{P} + \text{p} & \text{for} \\ \text{P} &= \text{p}_1 + \text{p}_2 & & ; & \text{p}_2 = \frac{1}{1+} \text{P} - \text{p} & \text{for} \quad N; \end{aligned} \quad (\text{B } 5)$$

(also p^0, P^0 for $\text{p}_1^0, \text{p}_2^0$), and

$$k^0 = \text{p} - \text{p}^0; \quad q^0 = \frac{1}{2} (\text{p} + \text{p}^0); \quad (\text{B } 6)$$

For the matrix element Eq. (B 4), the spatial part of the GCM kernel in Eq. (B 3) is calculated to be

$$\begin{aligned} G^{\text{space}}(\text{a}; \text{b}) &= \frac{1}{(2)^6} \frac{4+}{3} \int \frac{3}{2} \int d\text{P} dk^0 dq^0 u(k^0; \text{q}^0; \text{P}) \\ &\quad \exp \left(\frac{1}{6} \frac{+4}{+1} \text{P}^2 - \frac{1}{2} \frac{+1}{+1} \text{q}^0 + \frac{1}{4} \text{k}^0 \right. \\ &\quad \left. + i(\text{a} - \text{b}) \text{q}^0 + \frac{1}{+1} \text{P} + i \frac{1}{2} (\text{a} + \text{b}) \text{k}^0 \right); \end{aligned} \quad (\text{B } 7)$$

If we use Eq. (B 7) in Eq. (B 2), we can perform the integrals over a and b and obtain two delta functions. Thus we can perform the integrals over k^0 and q^0 and obtain the compact formula

$$\begin{aligned} V^{\text{space}}(\text{q}_f; \text{q}_i) &= e^{\frac{3}{32} \text{k}^2} \frac{2}{3} \int d\text{P} e^{\frac{2}{3} (\text{P} - \frac{3}{4} \text{q}^0)^2} \\ &\quad u(k; \text{q}) \frac{1}{+1} \text{P} \quad ; \end{aligned} \quad (\text{B } 8)$$

where $k = q_f - q_i$ and $q = (1/2) (q_f + q_i)$.

For a simple local Gaussian interaction with $u(r) = e^{-r^2}$ and $u(r)P_r$, we find

$$u(k; q; P) = -\frac{3}{2} \exp\left(-\frac{k^2}{4}\right) \quad \text{for } u(r) = e^{-r^2};$$

$$u(k; q; P) = -\frac{3}{2} \exp\left(-\frac{1}{q + \frac{1}{2} \frac{1}{P^2}}\right) \quad \text{for } u(r) = e^{-r^2} P_r; \quad (B9)$$

Then the P integral is carried out easily and we obtain

$$V_d(q_f; q_i) = -\frac{3}{2} \exp\left(-\frac{1}{4}\right) \frac{3}{8} + \frac{1}{4} k^2$$

$$\text{for } u(r) = e^{-r^2}; \quad (B10a)$$

$$V_e(q_f; q_i) = \frac{8}{3} \frac{1}{1 + \frac{8}{3}} \exp\left(-\frac{3}{32} k^2\right)$$

$$\frac{25}{24} \frac{1}{1 + \frac{8}{3}} q^2 \quad \text{for } u(r) = e^{-r^2} P_r; \quad (B10b)$$

If we further incorporate the spin-isospin factors, the full $V(q_f; q_i)$ is given by

$$V(q_f; q_i) = X_d V_d(q_f; q_i) + X_e V_e(q_f; q_i); \quad (B11)$$

with the spin-isospin factors defined by

$$\begin{aligned} X_d &= h \frac{X^5}{j!} \frac{!_d}{!_j} \frac{!_j}{!_2} \dots \frac{!_1}{!_1} \dots \frac{!_i}{!_i} \\ X_e &= \dots \end{aligned} \quad (B12)$$

Here h is the spin-isospin wave function of the α -cluster. The partial wave decomposition of Eq. (B10) is given by

$$V^d(q_f; q_i; i) = -\frac{3}{2} \exp\left(-\frac{1}{4}\right) \frac{3}{8} + \frac{1}{4} q_f^2 + q_i^2 \quad i = \frac{1}{2}, \frac{3}{8} + \frac{1}{4} q_f q_i; \quad (B13a)$$

$$V^e(q_f; q_i; i) = \frac{8}{3} \frac{1}{1 + \frac{8}{3}} \exp\left(-\frac{3}{32} q_f^2 - \frac{25}{24} \frac{1}{1 + \frac{8}{3}} q_i^2\right) \quad i = \frac{1}{2}, \frac{3}{8} + \frac{25}{24} \frac{1}{1 + \frac{8}{3}} q_f q_i; \quad (B13b)$$

where $i(x) = i' j'(ix)$ is the spherical Bessel function of imaginary argument.

APPENDIX C : BORN KERNEL OF THE RGM KERNEL

The Born kernels of the RGM kernel are directly derived from the effective two-nucleon force in the momentum representation, by using the method in Appendix A of Ref. [59]. We assume a central two-nucleon force, $v_{\text{central}} = v_0 e^{-r^2} (W + B P - H P - M P P)$, and the cut-off Coulomb force in Eq. (38). The spin-isospin factors for various interaction types of the interaction kernel are expressed only by two factors $X_d = 8W + 4(B - H) - 2M$ and $X_e = 8M + 4(H - B) - 2W$. These are given in Ref. [61] with respect to the exchange nucleon number x and the interaction type T . The internal energy of the α -cluster is given by

$$E^{\text{int}} = \frac{9\omega^2}{2M_N} + v_0 (X_d + X_e) \frac{r^2}{r} + 2e^2 - 1 - e^{-R^2/c^2}; \quad (C1)$$

The Born kernels are functions of k^2 , q^2 and $k \cdot q$ with $k = q_f - q_i$, $q = (q_f + q_i)/2$, and expressed by various spatial functions $f_{xT}(\cdot)$. Only with $\cos \theta = q_f \cdot q_i$ is explicitly written in $f_{xT}(\cdot)$, although these are also functions of q_f^2 and q_i^2 . The S^0 -type function $f_{xS^0}(\cdot)$ is obtained from $f_{xS}(\cdot)$ with k replaced by k . The partial wave decomposition of the Born kernel is carried out numerically through

$$f_{xT} = \frac{1}{2} \sum_{i=1}^{Z_1} f_{xT}(\cdot) P_i(\cos \theta) d(\cos \theta); \quad (C2)$$

The exchange normalization kernel is given by

$$K(q_f; q_i) = 4f_1(\cdot) - 3f_2(\cdot); \quad (C3)$$

with

$$f_1(\cdot) = \frac{r}{3} \frac{!_3}{b} \exp\left(-\frac{b^2}{2}\right) \frac{1}{3} q^2 + \frac{3}{4} k^2; \quad (C4)$$

$$f_2(\cdot) = \frac{p}{2} \frac{!_3}{b} \exp\left(-\frac{b^2}{2}\right) q^2 + \frac{1}{4} k^2; \quad (C4)$$

where the range parameter $b = \frac{p}{2}$ is used, instead of the width parameter w . The exchange kinetic-energy kernel is given by

$$G^K = \frac{3\pi^2}{4M_N b^2} 4f_1(1) 1 \frac{b^2}{3} \frac{4}{3} q^2 + k^2 \\ 3f_2(1) 1 \frac{2b^2}{3} q^2 + \frac{1}{4} k^2 \quad : \quad (C 5)$$

The direct potential is given by

$$V_D(q_f; q_i) = 2v_0 X_d - \frac{3}{8} b^2 \exp \frac{3}{8} b^2 + \frac{1}{4} k^2 \quad : \quad (C 6)$$

The direct Coulomb kernel is given by

$$V_D^{CL}(q_f; q_i) = 8 e^2 R_C^{-2} \frac{2}{k R_C} \sin \frac{k R_C}{2}^2 \exp \frac{3}{8} b^2 k^2 \quad : \quad (C 7)$$

The exchange interaction kernel is given by

$$G^V(q_f; q_i) = v_0 f_4(X_d + X_e) [f_{1E}(1) f_{1S}(1) \\ f_{1S^0}(1) - 2(2X_d - X_e) f_{1D+}(1) + 2X_e f_{1D}(1) \\ + 4(X_d + X_e) [f_{2E}(1) + f_{2S}(1) + f_{2S^0}(1)] \\ + (X_d - 2X_e) f_{2D+}(1) + f_{2D}(1)] \quad ; \quad (C 8a)$$

where

$$f_{1T}^8(1) = f_1(1) \\ \frac{1}{1+2b^2}^{\frac{3}{2}} \\ \frac{3}{3+8b^2}^{\frac{3}{2}} \exp \frac{n}{3+8b^2} \frac{b^2}{4} \frac{2}{3} q + k^2 \quad 1S \\ \frac{1}{1+4b^2}^{\frac{3}{2}} \exp \frac{n}{1+4b^2} \frac{b^2}{4} k^2 \quad 1D+ \\ \frac{3}{3+8b^2}^{\frac{3}{2}} \exp \frac{n}{3+8b^2} \frac{4}{9} b^2 q^2 \quad 1D \quad ; \quad (C 8b)$$

and

$$f_{2T}^8(1) = f_2(1) \\ \frac{1}{1+2b^2}^{\frac{3}{2}} \\ \frac{2}{2+5b^2}^{\frac{3}{2}} \exp \frac{n}{2+5b^2} \frac{b^2}{4} q + \frac{1}{2} k^2 \quad 2S \\ \frac{1}{1+3b^2}^{\frac{3}{2}} \exp \frac{n}{1+3b^2} \frac{b^2}{4} b^2 k^2 \quad 2D+ \\ \frac{1}{1+3b^2}^{\frac{3}{2}} \exp \frac{n}{1+3b^2} \frac{b^2}{4} b^2 q^2 \quad 2D \quad ; \quad (C 8c)$$

The exchange Coulomb kernel is given by

$$G^{CL}(q_f; q_i) = \frac{r}{h} \frac{e^2 n}{b} 4 f_{1E}^{CL}(1) f_{1S}^{CL}(1) f_{1S^0}^{CL}(1) 10 f_{1D+}^{CL}(1) 2 f_{1D}^{CL}(1) \\ + 4 f_{2E}^{CL}(1) + f_{2S}^{CL}(1) + f_{2S^0}^{CL}(1) + f_{2D+}^{CL}(1) + f_{2D}^{CL}(1) \quad ; \quad (C 9a)$$

where

$$f_{1T}^{CL}(1) = f_1(1) \\ \frac{1}{p\frac{3}{2}} \exp \frac{3}{32} b^2 \frac{2}{3} q + k^2 \frac{1}{h} \frac{1}{4} \frac{3}{2} b \frac{2}{3} q + k j \frac{1}{i} \frac{1}{2} \frac{3}{2} \frac{R_c}{b} \frac{1}{4} \frac{3}{2} b \frac{2}{3} q + k j \quad 1E \\ \frac{1}{p\frac{3}{2}} \exp \frac{1}{4} b^2 k^2 \frac{1}{h} \frac{1}{2} b k j \frac{1}{g} \frac{1}{2} \frac{R_c}{b} \frac{1}{2} b k j \quad 1S \\ \frac{1}{p\frac{3}{2}} \exp \frac{1}{6} b^2 k^2 \frac{1}{h} \frac{1}{6} b k j \frac{1}{g} \frac{1}{2} \frac{3}{2} \frac{R_c}{b} \frac{1}{6} b k j \quad 1D+ \\ \frac{1}{p\frac{3}{2}} \exp \frac{1}{6} b^2 k^2 \frac{1}{h} \frac{1}{6} b k j \frac{1}{g} \frac{1}{2} \frac{3}{2} \frac{R_c}{b} \frac{1}{6} b k j \quad 1D \quad ; \quad (C 9b)$$

and

$$f_{2T}^{CL}(1) = f_2(1) \\ \frac{1}{q\frac{5}{2}} \exp \frac{b^2}{n^{10}} q + \frac{1}{h} \frac{1}{2} k^2 \frac{1}{h} \frac{b}{10} j + \frac{1}{2} k j \frac{1}{g} \frac{2}{5} \frac{R_c}{b} \frac{b}{10} j + \frac{1}{2} k j \quad 2E \\ \frac{1}{q\frac{3}{2}} \exp \frac{b^2}{n^{12}} k^2 \frac{1}{h} \frac{b}{2} k j \frac{1}{g} \frac{1}{3} \frac{R_c}{b} \frac{b}{2} k j \quad 2S \\ \frac{1}{q\frac{3}{2}} \exp \frac{b^2}{3} q^2 \frac{1}{h} \frac{b}{3} j \frac{1}{g} \frac{1}{3} \frac{R_c}{b} \frac{b}{3} j \quad 2D+ \\ \frac{1}{q\frac{3}{2}} \exp \frac{b^2}{3} q^2 \frac{1}{h} \frac{b}{3} j \frac{1}{g} \frac{1}{3} \frac{R_c}{b} \frac{b}{3} j \quad 2D \quad ; \quad (C 9c)$$

Here, $\tilde{F}_0(x)$ and $g(x; \rho)$ are expressed by the Dawson integral or the error function of complex argument:

$$\begin{aligned}\tilde{F}_0(x) &= e^{-x^2} \int_0^x e^{x^2 t^2} dt = \frac{e^{-x^2}}{x} \int_x^\infty e^{u^2} du; \\ g(x; \rho) &= \tilde{F}_0(\rho) = \frac{\operatorname{erf}(x + i\rho)}{\operatorname{erf}(i\rho)} = \frac{1}{2} e^{-\rho^2} = \operatorname{erf}(x + i\rho) \quad \text{with} \quad \operatorname{erf}(z) = \frac{2}{\sqrt{\pi}} \int_0^z e^{-t^2} dt; \quad (C10)\end{aligned}$$

[1] S. Saito, *Prog. Theor. Phys. Suppl.* 62, 11 (1977).

[2] E. W. Schmid, *Z. Phys. A* 297, 105 (1980).

[3] H. Kamada and S. Oryu, *Prog. Theor. Phys.* 76, 1260 (1986).

[4] S. Oryu and H. Kamada, *Nucl. Phys. A* 493, 91 (1989).

[5] S. Oryu, K. Samata, T. Suzuki, S. Nakamura, and H. Kamada, *Few-Body Systems* 17, 185 (1994).

[6] H. Horiochi, *Prog. Theor. Phys.* 53, 447 (1975).

[7] E. Hiyama, M. Kamimura, T. Motoba, T. Yamada, and Y. Yamamoto, *Prog. Theor. Phys.* 97, 881 (1997).

[8] Y. Fujiwara, M. Kohno, and Y. Suzuki, to appear in *Few-Body Systems* (2003), nucl-th/0310028 and its revised version.

[9] E. M. Tursunov, D. Baye, and P. Descouvemont, *Nucl. Phys. A* 723, 365 (2003).

[10] P. Descouvemont, C. Daniel, and D. Baye, *Phys. Rev. C* 67, 044309 (2003).

[11] B. Buck, H. Friedrich, and C. W. Heatley, *Nucl. Phys. A* 275, 246 (1977).

[12] S. Ali and A. R. Bodmer, *Nucl. Phys.* 80, 99 (1966).

[13] Y. Fujiwara, M. Kohno, and Y. Suzuki, *Phys. Rev. C* 69, 037002 (brief report) (2003).

[14] Y. Fujiwara, H. Nemura, Y. Suzuki, K. Miyagawa, and M. Kohno, *Prog. Theor. Phys.* 107, 745 (2002).

[15] Y. Fujiwara, Y. Suzuki, K. Miyagawa, M. Kohno, and H. Nemura, *Prog. Theor. Phys.* 107, 993 (2002).

[16] Y. Fujiwara, K. Miyagawa, M. Kohno, Y. Suzuki, and H. Nemura, *Phys. Rev. C* 66, 021001(R) (2002).

[17] Y. Fujiwara, C. Nakamoto, and Y. Suzuki, *Phys. Rev. Lett.* 76, 2242 (1996); *Phys. Rev. C* 54, 2180 (1996).

[18] Y. Fujiwara, T. Fujita, M. Kohno, C. Nakamoto, and Y. Suzuki, *Phys. Rev. C* 65, 014002 (2002).

[19] Y. Fujiwara, K. Miyagawa, Y. Suzuki, M. Kohno, and H. Nemura, *Nucl. Phys. A* 721, 983c (2003).

[20] R. Machleidt, *Adv. Nucl. Phys.* 19, 189 (1989).

[21] A. Nogga, H. Kamada, and W. G.lockle, *Phys. Rev. Lett.* 85, 944 (2000).

[22] Y. Fujiwara, K. Miyagawa, M. Kohno, and Y. Suzuki, KUNS-1907, nucl-th/0404010, submitted to *Phys. Rev. C*.

[23] P. M. M. Maessen, Th. A. Rijken, and J. J. de Swart, *Phys. Rev. C* 40, 2226 (1989).

[24] Th. A. Rijken, V. G. J. Stoks, and Y. Yamamoto, *Phys. Rev. C* 59, 21 (1999).

[25] H. Bando, K. Ikeda, and T. Motoba, *Prog. Theor. Phys.* 69, 918 (1983).

[26] W. Buckner et al., *Phys. Lett.* 55B, 107 (1975).

[27] M. May et al., *Phys. Rev. Lett.* 51, 2085 (1983).

[28] D. H. D avis and J. Pniewski, *J. Contemp. Phys.* 27, 91 (1986).

[29] D. H. D avis, *LAMPF Workshop on (;K) Physics*, edited by B. F. Gibson, W. R. Gibbs, and M. B. Johnson, *AIP Conference Proceedings* 224, New York, 1991, p. 38.

[30] H. Bando, T. Motoba, and J. Zofka, *Int. J. Mod. Phys. A*, 5, 4021 (1990).

[31] H. Akikawa et al., *Phys. Rev. Lett.* 88, 082501 (2002).

[32] E. Hiyama, M. Kamimura, T. Motoba, T. Yamada, and Y. Yamamoto, *Phys. Rev. Lett.* 85, 270 (2000).

[33] Y. Yamamoto and Bando, *Prog. Theor. Phys.* 69, 1312 (1983).

[34] I. N. Filikhin and A. Gal, *Nucl. Phys. A* 707, 491 (2002).

[35] I. Kumagai-Fuse, S. Okabe, and Y. Akaishi, *Phys. Lett. B* 345, 386 (1995).

[36] S. Oryu, H. Kamada, H. Sekine, H. Yamashita, and M. Nakazawa, *Few-Body Systems* 28, 103 (2000).

[37] Y. Koike (private communication).

[38] Y. Fukushima and M. Kamimura, *Suppl. to J. Phys. Soc. Jpn.* 44, 225 (1978).

[39] E. Uegaki, S. Okabe, Y. Abe, and H. Tanaka, *Prog. Theor. Phys.* 57, 1262 (1977); *ibid.* 62, 1621 (1979).

[40] P. Descouvemont and D. Baye, *Phys. Rev. C* 36, 54 (1987).

[41] J.-M. Spaerenberg and D. Baye, *Phys. Rev. C* 55, 2175 (1997).

[42] W. G.lockle, *The Quantum Mechanical Few-Body Problem*, *Texts and Monographs in Physics*, (Springer, Berlin, 1983).

[43] D. R. Thompson, M. Lemer, and Y. C. Tang, *Nucl. Phys. A* 286, 53 (1977).

[44] Y. Fujiwara, M. Kohno, C. Nakamoto, and Y. Suzuki, *Phys. Rev. C* 64, 054001 (2001).

[45] R. H. Dalitz, R. C. Hemandon, and Y. C. Tang, *Nucl. Phys. B* 47, 109 (1972).

[46] H. Bando and I. Shimodaya, *Prog. Theor. Phys.* 63, 1812 (1980).

[47] H. Nemura, Y. Akaishi, and Y. Suzuki, *Phys. Rev. Lett.* 89, 142504 (2002).

[48] M. Kohno, Y. Fujiwara, and Y. Akaishi, *Phys. Rev.* 68, 034302 (2003).

[49] Y. Fujiwara, M. Kohno, C. Nakamoto, and Y. Suzuki, *Prog. Theor. Phys.* 104, 1025 (2000).

[50] A. B. Volkov, *Nucl. Phys.* 74, 33 (1965).

[51] Y. Suzuki and H. Matsumura (private communication).

[52] C. M. Vincent and S. C. Phatak, *Phys. Rev. C* 10, 391 (1974).

[53] W. G.lockle, G. Hasberg, and A. R. Negehabian, *Z. Phys. A* 305, 217 (1982).

[54] See ARPACK homepage, <http://www.caam.rice.edu/software/ARPACK/>

[55] J. A. Koepke, R. E. Brown, Y. C. Tang, and D. R.

Thompson, Phys. Rev. C 9, 823 (1974).

[56] Y. Fujiwara, H. Horiuchi, K. Ikeda, M. Kamimura, K. Kato, Y. Suzuki, and E. Udegaki, Prog. Theor. Phys. Suppl. 68, 29 (1980).

[57] Y. Yamamoto, T. Motooba, H. Hideno, K. Ikeda, and S. Nagata, Prog. Theor. Phys. Suppl. 117, 361 (1994).

[58] H. Takahashi et al. (KEK-PS E373 collaboration), Phys. Rev. Lett. 87, 212502 (2001).

[59] Y. Fujiwara, M. Kohno, T. Fujita, C. Nakamoto, and Y. Suzuki, Prog. Theor. Phys. 103, 755 (2000).

[60] C. Nakamoto, Y. Suzuki, and Y. Fujiwara, Prog. Theor. Phys. 94, 65 (1995).

[61] Y. Fujiwara and Y. C. Tang, Memoirs of the Faculty of Science, Kyoto University, Series A of Physics, Astrophysics, Geophysics and Chemistry, 39, No. 1, Article 5 (Faculty of Science, Kyoto University, Kyoto, 1994), p. 91.